Distribution Agreement

In presenting this thesis or dissertation as a partial fulfillment of the requirements for an advanced degree from Emory University, I hereby grant to Emory University and its agents the non-exclusive license to archive, make accessible, and display my thesis or dissertation in whole or in part in all forms of media, now or hereafter known, including display on the world wide web. I understand that I may select some access restrictions as part of the online submission of this thesis or dissertation. I retain all ownership rights to the copyright of the thesis or dissertation. I also retain the right to use in future works (such as articles or books) all or part of this thesis or dissertation.

Signature:

_____ _____

Roger Park   Date

The Catalytic Aerobic Oxidation of Aldehyde and Alcohol Substrates with Redox-

Active Ligand-Supported Earth-Abundant Metal Catalysts

By
Roger Park
Master of Science
Chemistry

_____
Cora E. MacBeth, Ph.D.
Advisor

_____
Huw M. L. Davies, Ph.D.
Co-Advisor

_____
Lanny S. Liebeskind, Ph.D.
Committee Member

_____
Christopher Scarborough, Ph.D.
Committee Member

Accepted:

_____
Lisa A. Tedesco, Ph.D.
Dean of the James T. Laney School of Graduate Studies

_____
Date

The Catalytic Aerobic Oxidation of Aldehyde and Alcohol Substrates with Redox-Active

Ligand-Supported Earth-Abundant Metal Catalysts

By

Roger Park

B.S. UC San Diego, 2012

Advisor: Cora E. MacBeth

An abstract of

A thesis submitted to the faculty of the

James T. Laney School of Graduate Studies of Emory University

In partial fulfillment of the requirements for the degree of Master of Science in Chemistry

2016

Abstract

The Catalytic Aerobic Oxidation of Aldehyde and Alcohol Substrates with Redox-Active Ligand-Supported Earth-Abundant Metal Catalysts

By Roger Park

This thesis describes the application of dinuclear earth-abundant metal complexes supported by the same redox-active ligand scaffold, L^{iPr}, towards the catalytic aerobic oxidation of two different substrate classes. The first section of this thesis covers the catalytic deformylation of aldehydes to form ketone products with $(Et_4N)_2[Co_2L_2{}^{iPr}]$. Efforts to probe the proposed nucleophilic character of the previously spectroscopically characterized Co^{III}-superoxide species via deformylations of 2-phenylpropionaldehyde derivatives featuring various steric and electronic traits are described. The second section of this thesis covers the aerobic oxidation of alcohols to form ketone and aldehyde products catalyzed by $(PPh_4)_2[Cu_2L_2{}^{iPr}]$ and di-*tert*-butyl azodicarboxylate (DBAD) as an organic co-catalyst. Preliminary studies suggest that $(PPh_4)_2[Cu_2L_2{}^{iPr}]$ is capable of catalytically oxidizing alcohol substrates as broad in scope as previously reported for Cu-DBAD co-catalyst systems.

The Catalytic Aerobic Oxidation of Aldehyde and Alcohol Substrates with Redox-Active

Ligand-Supported Earth-Abundant Metal Catalysts

By

Roger Park

B.S. UC San Diego, 2012

Advisor: Cora E. MacBeth

A thesis submitted to the Faculty of the

James T. Laney School of Graduate Studies of Emory University

in partial fulfillment of the requirements for the degree of

Master of Science

in Chemistry

2016

Table of Contents

List of Figures, Tables, and Schemes

List of Tables   **Page**

List of Schemes   **Page**

LIST OF ABBREVIATIONS

GO: galactose oxidase

Tyr: tyrosine

AD: aldehyde decarbonylase

CYP: cytochrome P450

cADO: cyanobacterial aldehyde decarbonylase

Xantphos: 4,5-bis(diphenylphosphino)-9,9-dimethylxanthene

dppp: diphenylphosphine

nbd: norbonadiene

nbe: norbornene

cod: cyclooctadiene

2-PPA: 2-phenylpropionaldehyde

CCA: cyclohexanecarboxaldehyde

TMC: tetraazamacrocyclam

Et_4N^+: tetraethylammonium

L^{iPr}: 2,2'-bis(isobutyrylamido)diphenylamine

L^{Me}: 2,2'-bis(methylamido)diphenylamine

L^{CF3}: 2,2'-bis(trifluoroacetamido)diphenylamine

EtOAc: ethyl acetate

KO^tBu: potassium *tert*-butoxide

Et_2O: diethyl ether

Et$_3$N: triethylamine

nBuLi: *n*-butyllithium

DMF: dimethylformamide

MeCN: acetonitrile

PCC: pyridinium chlorochromate

DBAD: di-*tert*-butyl azodicarboxylate

TEMPO: (2,2,6,6-tetramethylpiperidin-1-yl)oxyl

PPh$_4^+$: tetraphenylphosphonium

I. General Introduction

Oxidation is an important process for converting chemical feedstocks into higher value-added commodity and fine chemicals. Unfortunately, the wide-scale application of oxidation reactions is commonly beset by the use of atom-inefficient stoichiometric equivalents of inorganic salts or hypervalent iodine reagents.[1] Their usage leads to toxic by-products whose disposal adds additional costs into the large-scale production of chemicals. The oxidation of alcohols to carbonyls, a ubiquitous transformation that permits access to more electrophilic carbon centers, is a rarely used reaction in the pharmaceutical industries precisely because of the complications posed by hazardous waste disposal. Indeed, a 2006 *Organic & Biomolecular Chemistry* report on R&D process chemistry methods reveals that oxidation is so often intentionally designed out of drug syntheses that it only comprises 3.9% of the total reactions performed by leading pharmaceutical firms.[2] There is consequently an ongoing search for new oxidants to enable greater flexibility in industrial chemical production methods.

Practically infinite in supply and usually only producing water as the by-product, atmospheric O_2 would be the obvious terminal oxidant of choice over the aforementioned reagents. Given the high activation barriers of O_2, however, catalysts would be needed to promote aerobic oxidation. Examples of such catalytic systems indeed already exist[3], and perhaps the most widely used catalytic aerobic oxidation reactions are the production of ethylene oxide from ethylene via silver compounds[4] and the production of carbonyls from alkenes via the Wacker process[5], as summarized in **Figure 1**. In either case, though, the key shortcoming is that although these production methods avoid using stoichiometric

oxidants, they still involve second- and third-row Group VIII-X metals, thus limiting their economic efficiency and sustainability.
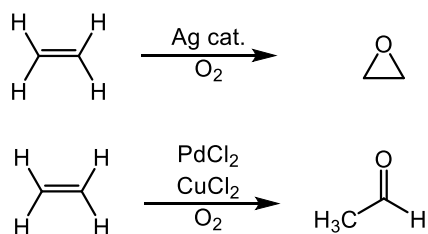
Figure 1. Industrial examples of aerobic oxidation. **Top:** Ethylene oxide produced from ethylene and silver catalysts.[4] **Bottom:** Aldehyde produced from ethylene via Wacker process.[5]

In order to address these challenges, it is crucial for chemists to invent new catalysts that not only employ O_2 as the terminal oxidant, but are also comprised of cheap, earth-abundant metals. Metals such as iron, cobalt, and copper are attractive not only for their extremely affordable prices in comparison to metals such as palladium, but also because their by-products are often far less environmentally hazardous than heavy metal wastes.

However, first-row transition metals are characterized by shorter ligand field splitting than their second- and third-row metal counterparts, and this causes first-row metals to typically exist in high-spin electron configurations. This causes them to operate via 1 e^- redox couples such as $Cu^{I/II}$ instead of the 2 e^- redox couples commonly exhibited by metals such as $Pd^{0/II}$, resulting in complications with controlling reactivity and catalyst stability.[6] Nature sometimes circumvents this impediment by supporting the metal centers of their enzymes with redox-active ligands to access multi-electron processes, as exemplified by galactose oxidase (*vide infra*).[7]

Whereas the metal's oxidation state in classic Werner complexes such as *cis*-[Co(NH$_3$)$_4$Cl$_2$]Cl are unambiguously defined because their ligands possess unchanging redox states[8], redox-active ligands are 'non-innocent' in the sense that they are capable of undergoing redox events, independent of the metal center they are coordinated to. As exemplified by Gray's analysis of bis(dithiolene)-supported nickel complexes (**Figure 2**), assuming ligand redox innocence leads to incorrect assignment of the nickel center's oxidation state.[9] Ligand non-innocence, then, permits a strategy of combining 1 e$^-$ transfers from the metal center with 1 e$^-$ transfers from the redox-active ligands to access the necessary multi-electron processes necessary to activate O$_2$ as a terminal oxidant.
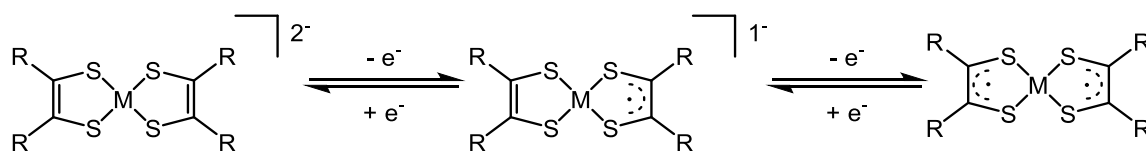
Figure 2. Redox-active bis(dithiolene) metal-ligand complexes.[9]

Galactose oxidase (GO) is one particularly illustrative example of a metalloenzyme that utilizes this strategy. GO catalytically oxidizes alcohols to aldehydes and generates H$_2$O$_2$ as a by-product in the presence of O$_2$. The catalytic cycle, as depicted in **Scheme 1**, involves the Tyr$_{272}$ ligand performing a 1 e$^-$ oxidation of the alcohol substrate along with the copper(II) center in a stepwise radical mechanism to lead to the final product.[7]
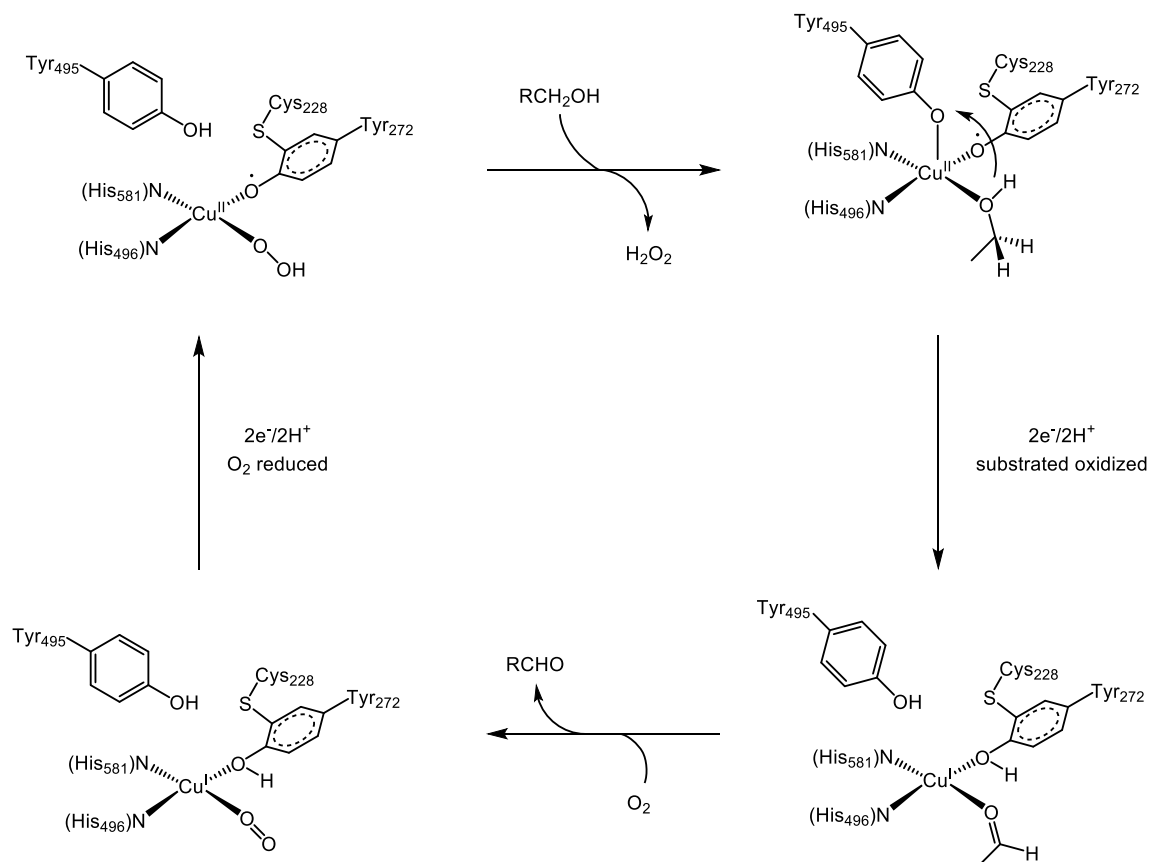
Scheme 1. Proposed mechanism of alcohol oxidation by galactose enzyme.[7]

As demonstrated by GO, nature has provided us with a template for developing sustainable, cost-effective catalysts. It is evident that the ideal catalyst will be capable of oxidizing organic feedstocks by activating O_2 with earth-abundant metals. Furthermore, to circumvent the complications that result from 1 e^- transfers, these metal centers must be supported by redox-active ligands to promote multi-electron processes. This thesis describes the application of cobalt- and copper-centered complexes supported by the same redox-active ligand scaffold towards two significant processes, the catalytic deformylation of aldehydes and the oxidation of alcohols, respectively.

II: Aerobic Aldehyde Deformylation Catalyzed by $(Et_4N)_2[Co_2L_2{}^{iPr}]$

A. INTRODUCTION

Nature features a class of diverse metalloenzymes called aldehyde decarbonylases (ADs), which catalyze the deformylation of aldehyde functionalities.[10] Interestingly, every AD known thus far is an oxygenase such as cytochrome P450 (CYP), which is well-known for its extraordinary ability to selectively hydroxylate C-H bonds in steroids with O_2 as the terminal oxidant.[11] Thus, the very enzymes that are typically thought of as functionalizing chemically inert C-H bonds are also capable of *de*functionalizing pre-functionalized organic substrates, as depicted in **Schemes 2** and **3**.
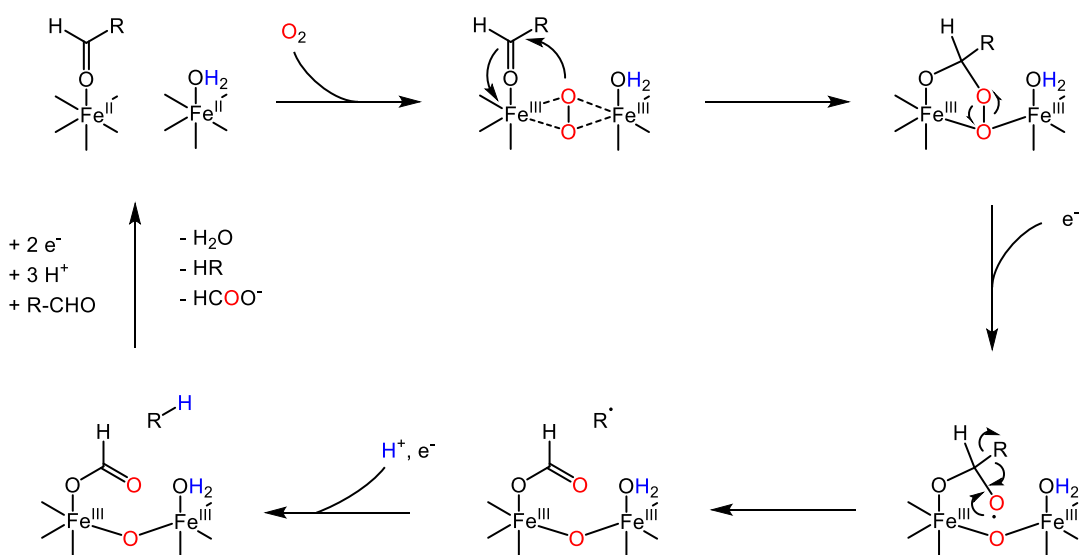
Scheme 2. Proposed mechanism for deformylation by cyanobacterial AD (cADO). Color-coded atoms were isotopically labeled to verify intermediates.[12]
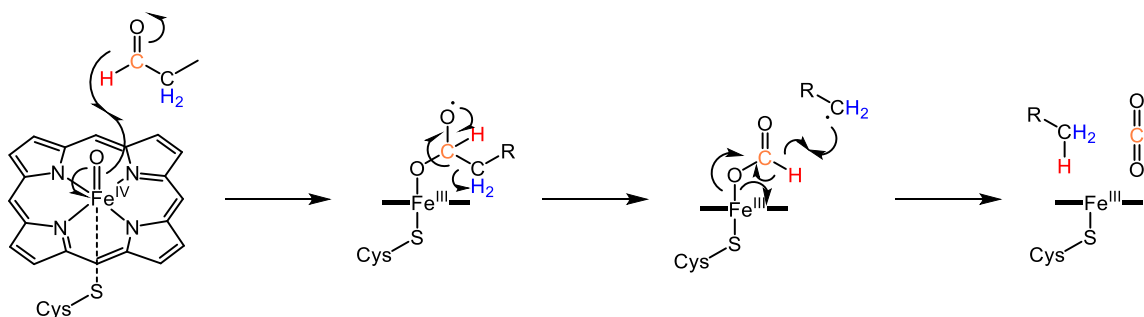
Scheme 3. Deformylation of fatty aldehydes by insect AD (CYP4G1). Color-coded atoms were isotopically labeled to verify intermediates.[13]

While it may not be immediately apparent why Nature would require avenues for defunctionalizing substrates, the products of deformylation reactions serve many important biological roles. For example, long-chain alkane products from deformylation serve as anti-desiccants in plants,[14] contact pheromones for insects,[15] and alternative energy sources for algae when insufficient light exists for photosynthesis.[16] In humans, placental aromatase synthesizes estrogen as shown in **Scheme 4** by converting the methyl group α to the ketene C-C double bond of an androgen substrate (**1**) to an aldehyde group (**3**), which is ultimately deformylated to yield the final product.[17]
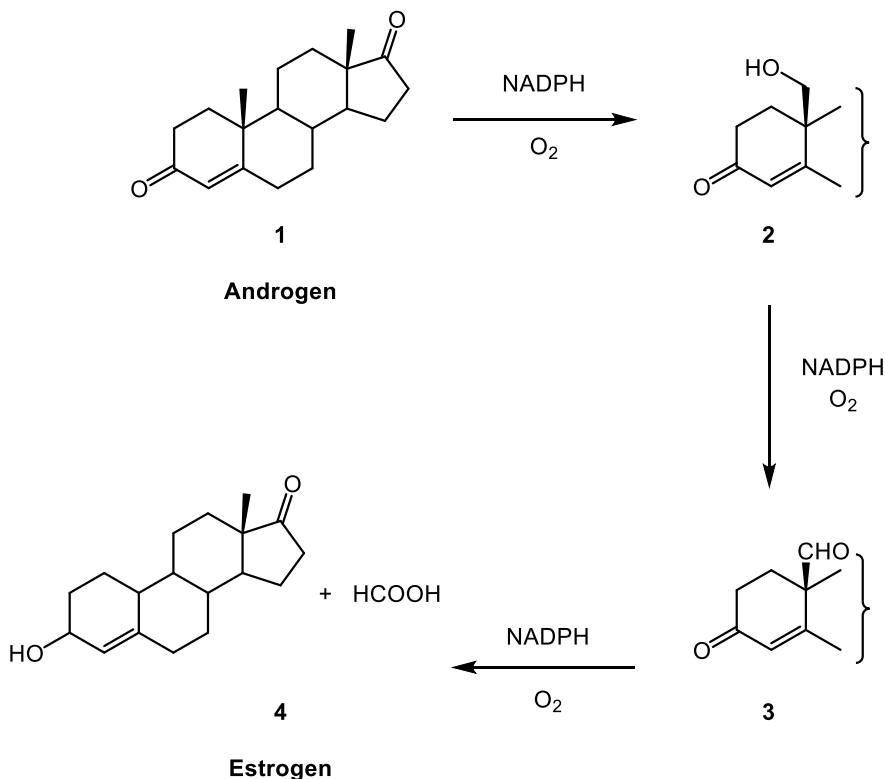
Scheme 4. Placental aromatase-catalyzed conversion of androgen (**1**) to estrogen (**4**) through an aldehyde intermediate (**3**).[17]

Catalytic deformylation possesses many potential applications for society. For example, the synthesis of long-chain alkanes from aldehydes for anti-dessicants for plants and energy reserves for algae has important implications for the conversion of biowaste into commodity chemicals and hydrocarbon fuel sources. Additionally, the conversion of androgen to estrogen by placental aromatase hints at future methodologies that selectively deformylate aldehydes for late-stage disconnection strategies in the synthesis of pharmacologically relevant molecules. Lastly, aldehyde deformylation can also serve to help probe what the active catalytic $M-O_2$ species is, and this may contribute to improved catalytic design when modifying a ligand scaffold to discriminate in favor of a specific $M-O_2$ configuration.

Efforts at developing deformylation catalysts to access these applications have been broadly divided into two separate approaches, organometallic and biomimetic. The field of organometallic deformylation catalysts first began in the 1960s, when Tsuji and Ohno discovered that Wilkinson's catalyst could deformylate aldehydes in addition to its more common application in hydrogenating olefins, although catalytic behavior was only observed at temperatures above 100 °C with low turnover numbers.[18] Doughty and Pinolet improved upon Tsuji and Ohno's work by utilizing chelating biphenylphosphine ligands for improved catalytic activity[19], and Madsen *et al* improved on this yet further in the late 2000's by developing a methodology for *in situ* catalyst synthesis.[20] Follow-up mechanistic studies by the Madsen group proposed a mechanism in which the aldehyde substrate's C-H bond oxidatively adds to the rhodium center to form a Rh-acyl complex, followed by migratory extrusion of the axial carbon monoxide ligand, and finally reductive elimination to release the product (**Scheme 5**).[21] Most recently, Dong *et al* have developed a rhodium (Xantphos)(benzoate) complex, which converts aldehydes to olefins at low catalyst loadings and mild temperatures.[22]
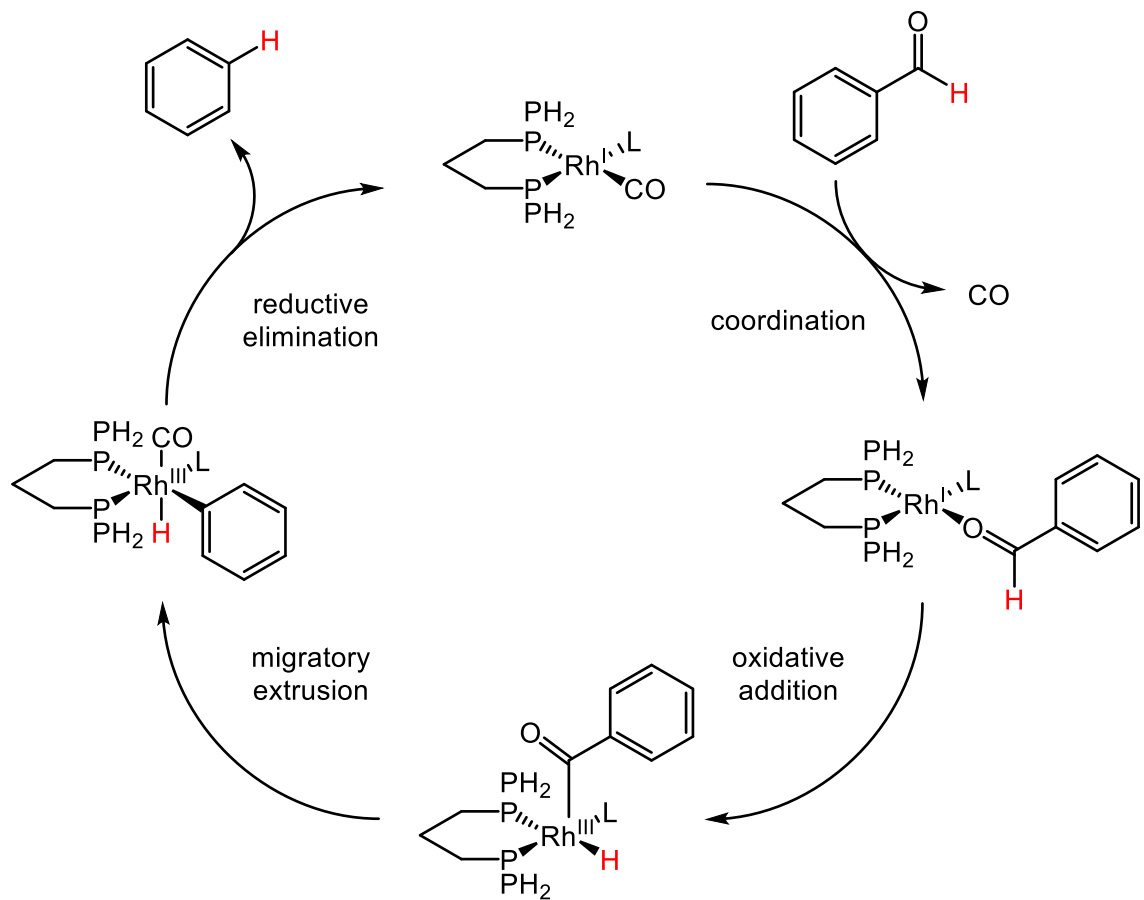
Scheme 5. Madsen's proposed catalytic mechanism of aldehyde deformylation by chelated rhodium complexes.[21]

A.

B.

$RhCl_3 \cdot 3H_2O$ $H_2PP \diagup\diagdown\diagup PPh_2$
dppp

C.

[Rh(cod)OMe]$_2$

Xantphos

nbd   or   nbe
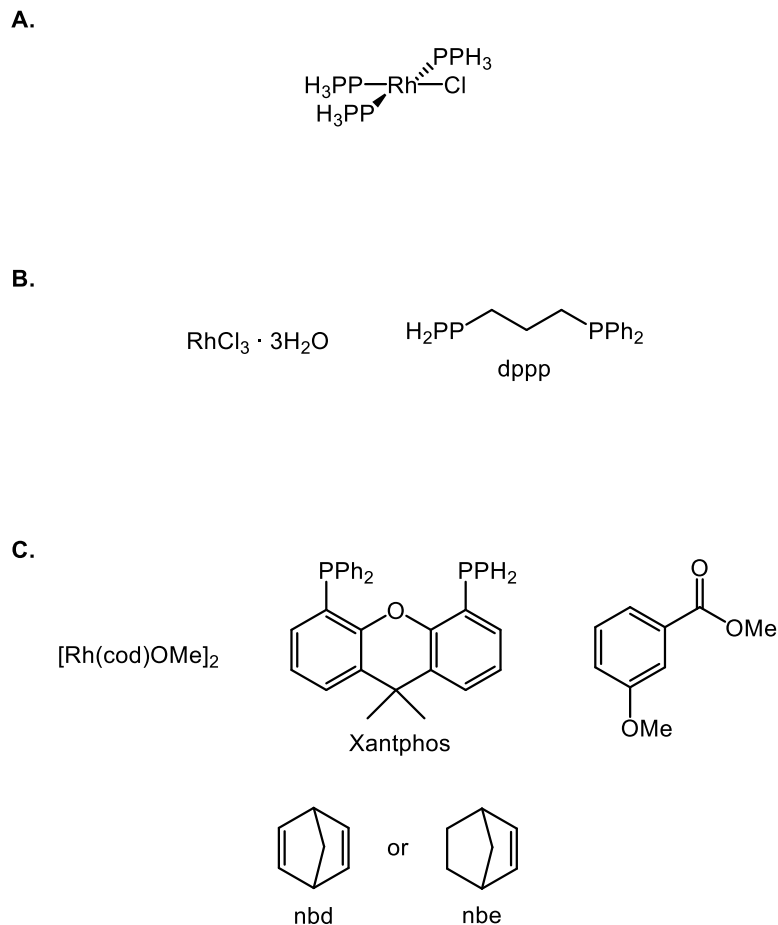
Figure 3. Examples of deformylation catalysts. **A)** Wilkinson's catalyst, first discovered by Tsuji and Ohno to be capable of catalytic behavior at elevated temperatures.[18] **B)** Chelating bis(diphenylphosphine)-supported rhodium complexes discovered to catalyze aldehyde deformylation at milder conditions.[19] **C)** Rhodium (Xantphos)(benzoate) complex, discovered by Dong *et al* to deformylate aldehydes to olefins.[22]

In every example listed thus far (**Figure 3**), however, the organometallic complex requires an expensive rhodium metal center. The observation that nature catalytically deformylates aldehydes with cheap, environmentally-benign first-row Group VIII-XI metal-centered catalysts and O$_2$ as the terminal oxidant, however, provides a tantalizing

future of developing biologically inspired complexes that catalyze deformylation through analogous first-row transition metal-O_2 adducts.

Indeed, the literature is rich with examples of such biologically inspired complexes. CYP mimics were designed by Valentine *et al* featuring a heme-supported ferric-peroxo species that were then characterized as nucleophilic by reacting them with electrophilic substrates such as acyl halides.[23] The oxidative nucleophilic reactivity of the ferric-peroxo complexes was further demonstrated by the deformylation of aldehyde substrates.[24] Nam *et al* built on this work through their studies of tetraazamacrocyclam (TMC) supported first-row metal complexes. By studying a family of various first-row metal-cyclam complexes and their reactivity towards the deformylation of 2-phenylpropionaldehyde (**2-PPA**) and cyclohexanecarboxaldehyde (**CCA**), the Nam group was able to identify the active metal-O_2 adduct catalyst as nucleophilic in character (**Scheme 6**).[25] Importantly, the work from Valentine and Nam demonstrates that catalytic deformylation can be achieved with first-row Group VIII-XI complexes that require neither a heme ferric-peroxo species nor a protein environment as in nature.
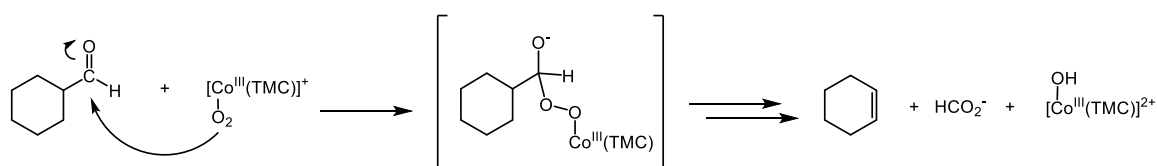
Scheme 6. Nam's [Co^{III}(TMC)]$^+$-O_2 adduct-catalyzed aldehyde deformylation of CCA to cyclohexene to probe the active catalyst species' nucleophilicity.[25]

The key shortcoming with Valentine and Nam's systems, however, is that the active nucleophilic metal-O_2 catalyst must be formed from either superoxide or peroxide sources, not O_2 (**Scheme 7**).[23a, 26] Utilizing O_2 would provide a more atom-economical,

cost-effective, and environmentally benign alternative terminal oxidant to these other oxygen atom sources.
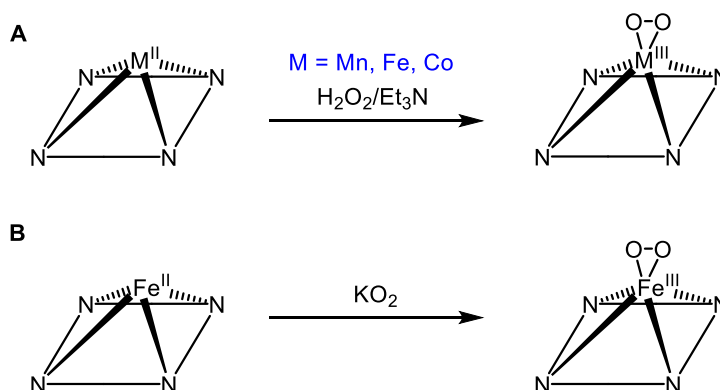
Scheme 7. A) Synthesis of TMC-supported M-O_2 adducts with H_2O_2.[26] **B)** Synthesis of porphyrin-supported M-O_2 adducts with KO_2.[23a]

Thus, a historical overview of the past 60 years in deformylation catalyst development suggests that further advancements are both needed and accessible. Namely, an ideal catalyst will consist of a first-row transition metal center that utilizes O_2 as the terminal oxidant to create the active metal-O_2 adduct catalyst for oxygenative deformylation of aldehyde substrates.

Previous work in our lab established that the complex **(Et₄N)₂[Co₂L₂^{iPr}]** (where L = N(o-PhNC(O)^{i}Pr)₂) catalyzes the oxidation of triphenylphosphine to triphenylphosphine oxide.[27] We hypothesized upon the basis of earlier spectroscopic studies with our collaborators that upon O_2 exposure, the complex rapidly breaks down from its pre-catalytic dimeric form to a catalytically active, mononuclear high-spin Co^{II}-superoxide species capable of oxygen atom transfer, as shown in **Scheme 8**.[28]

A.

B.
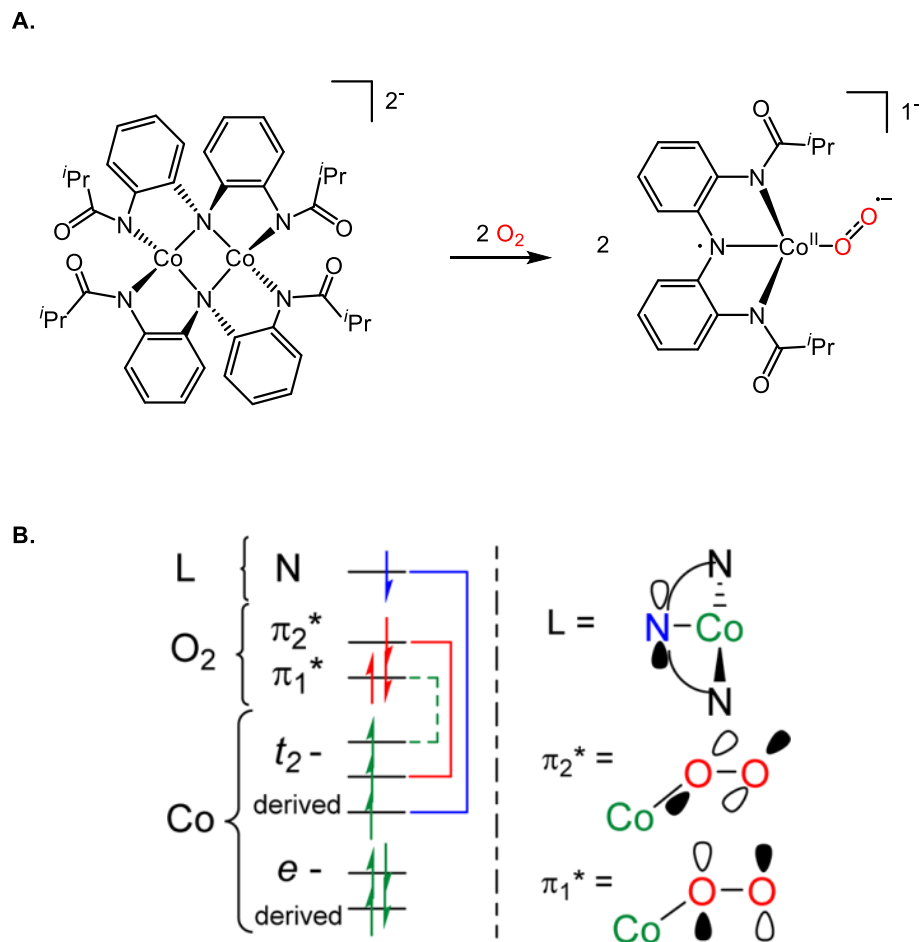
Scheme 8. A) Preparation of high-spin monomeric Co^{II}-superoxide from **$(Et_4N)_2[Co_2L_2{}^{iPr}]$** pre-catalyst dimer. **B)** Molecular orbital diagram of the catalytically active high-spin Co^{II}-superoxide monomer.[28]

We were interested in evaluating whether this monomeric M-O_2 adduct is capable of oxidizing other organic substrates and therefore investigated its potential for aldehyde deformylation, with biological precedence from the aforementioned AD enzymes that similarly catalyze aldehyde deformylation via M-O_2 adducts. The first portion of this report therefore details the application of a redox-active ligand-supported cobalt complex towards catalytic aldehyde deformylation through activation by O_2. The synthesis of the

methyl derivative of this ligand platform, and its metalation with cobalt to study the influence of reduced steric encumbrance on aldehyde deformylation are also described.

B. RESULTS AND DISCUSSION

A series of redox-active amidate ligands were prepared according to the route depicted in **Scheme 9**, which provides the versatility of incorporating various substituents to explore steric and electronic effects. The ligand [HN(o-PhNHC(O)^{i}Pr)$_2$] (**H$_3$L^{iPr}**) was prepared according to previously reported procedures.[29] [HN(o-PhNHC(O)CF$_3$)$_2$] (**H$_3$L^{CF3}**) was also prepared to investigate the influence of electron-withdrawing ligand substituents on catalytic activity, with the expectation that the cobalt catalyst bearing this ligand would exhibit reduced reactivity towards aldehyde substrates than **(Et$_4$N)$_2$[Co$_2$L$_2$^{iPr}]** due to decreased nucleophilicity. Finally, the methyl derivative, [HN(o-PhNHC(O)Me)$_2$] (**H$_3$L^{Me}**), was prepared for the first time in order to investigate the influence of reduced steric hindrance on the kinetics of catalysis in comparison to the more sterically encumbered **H$_3$L^{iPr}**.
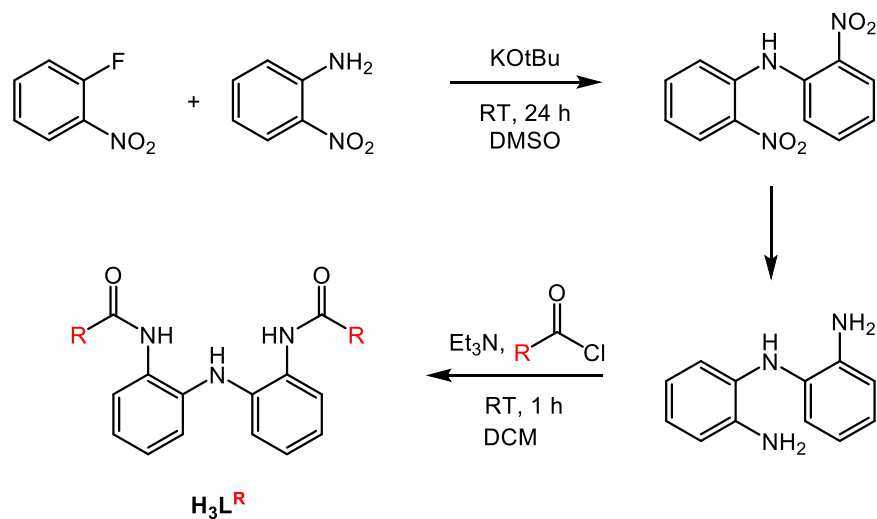
Scheme 9. Synthesis of HN(*o*-PhNHC(O)R)$_2$ (**H$_3$L^R**).
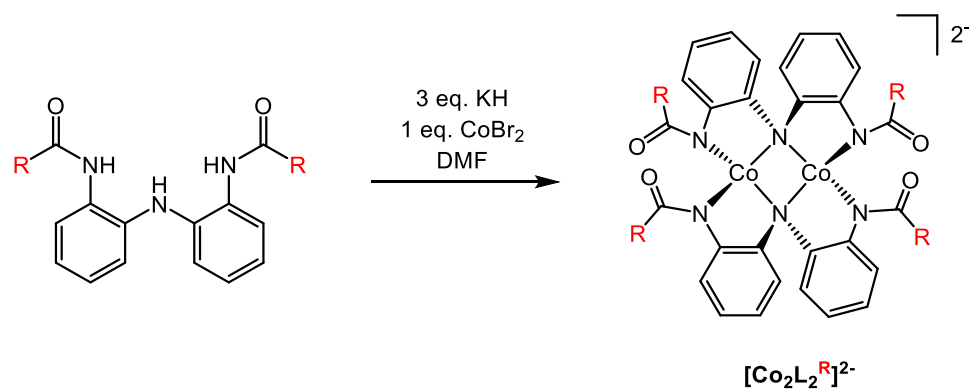
Scheme 10. Synthesis of **[Co$_2$L$_2$^{R}]$^{2-}$**.

(**Et$_4$N)$_2$[Co$_2$L$_2$^{iPr}]**, synthesized as depicted in **Scheme 10**, was first investigated towards catalytic deformylation with **2-PPA** as the model substrate, where acetophenone is predicted to be the main product. At a 5 mol% catalyst loading, the reaction led to an isolable 91% yield of acetophenone as product, as determined by NMR. The reaction proceeds at room temperature under 1 atm O$_2$ and is essentially complete (as determined by consumption of substrate in GC-MS) within 24 hours. This marks the first known example of deformylation by a synthetic catalyst that was activated by O$_2$, not superoxide

or peroxide reagents. Although GC-MS of the reaction mixture indicated complete consumption of **2-PPA**, it also revealed minor formation of an unknown product with a *m/z* of 120. While the identity of this minor product has yet to be determined, styrene oxide, the most obvious possible product with similar *m/z*, was ruled out by comparison of the GC-MS spectrum of an authentic sample of styrene oxide. With increase of the catalyst loading to 10 mol%, the formation of this unknown product was suppressed and only the acetophenone product was formed. Thus, all other exploratory deformylation reactions were run at 10 mol% catalyst loading to avoid any other potential side reaction (**Scheme 11**).

2-phenylpropionealdehyde
(**2-PPA**)

$(Et_4N)_2[Co_2L_2{}^{iPr}]$ (10 mol%)

O_2, MeCN
RT, 24 h.

acetophenone
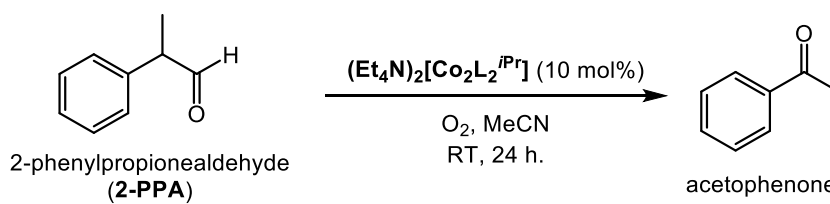
Scheme 11. Catalytic deformylation reaction conditions of **2-PPA**. Yield was 91% as determined by isolable conversion of substrate.

Studies were expanded to other aldehyde substrates to see if they could similarly be catalytically deformylated (see **Table 1**). Entries **A-C** were selected as biologically relevant compounds that would provide an early proof-of-concept demonstration that deformylation could be applied in a late stage synthesis, akin to nature's synthesis of estrogen from androgen.
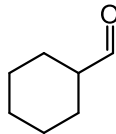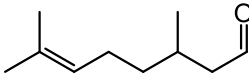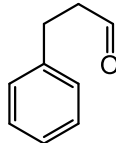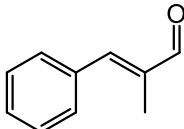
Entry	Substrate
CCA	
A	
B	
C	

Table 1. Aldehyde substrates tested for catalytic deformylation. *Reaction conditions:* In a typical procedure, 10 mol% of $(Et_4N)_2[Co_2L_2{}^{iPr}]$ and 1 mol. equivalent of substrate were dissolved in dry acetonitrile inside a glove box. The reaction mixture was then removed from the glove box and briefly evacuated of N_2 under a vacuum line. The reaction was then stirred for 24 hrs. under positive O_2 flow at 1 atm. The following day, an aliquot was removed from the reaction mixture, diluted in excess dichloromethane and then filtered through a plug of silica. The solution was then submitted for GC-MS analysis.

Cyclohexanecarboxaldehyde (**CCA**) is another biologically relevant substrate that is deformylated by $P240_{2B4}$, a liver P450 enzyme, to produce cyclohexene and formic acid. As seen in **Scheme 12**, the mechanism of **CCA** deformylation involves

nucleophilic attack by a side-on metal-peroxo intermediate to form a 6-membered pericyclic intermediate that then leads to formation of the final products. Notably, this specific mechanism requires an external proton source and a β-H atom in order for the reaction to proceed.[30] 2-phenylpropionealdehyde (**2-PPA**), on the other hand, lacks a β-H atom, thus deformylation cannot proceed via this mechanism. However, it is successfully deformylated to a ketone rather than an alkene, *without* an external proton source, indicating that it does not undergo deformylation through a $P240_{2B4}$-like mechanism. Thus, **CCA** in conjunction with **2-PPA** serve as useful substrates for probing mechanistic pathways through which the catalyst operates.
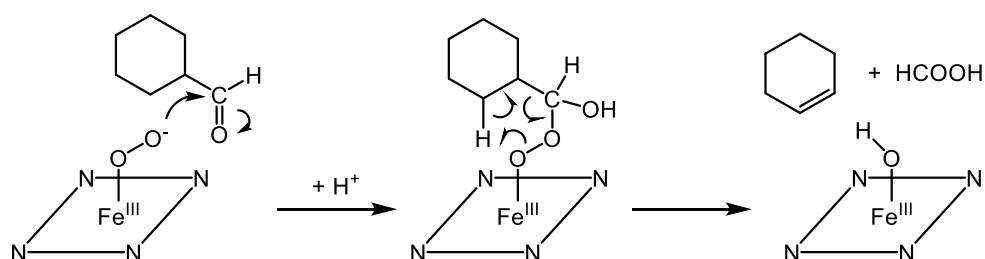
Scheme 12. CCA deformylation catalyzed by $P240_{2B4}$.[30]

Substrates **A-C** did not display catalytic turnover with $(Et_4N)_2[Co_2L_2{}^{iPr}]$ and only returned starting material. Control experiments also established that **CCA** readily oxidizes to a mixture of products in the presence of O_2 without catalyst. Thus, solvent and temperature conditions for the reaction were varied in efforts to suppress this background oxidation in favor of catalysis and/or bypassing a higher thermodynamic barrier posed by **CCA**. However, these attempts at optimization were not successful in identifying reaction conditions to promote selective oxidation of **CCA** by the catalyst, and the results suggest that $(Et_4N)_2[Co_2L_2{}^{iPr}]$ does not catalytically deformylate **CCA** (see **Figure 6** in Experimental).

These results may be justified by recent work from McDonald *et al* that hypothesizes that aldehyde deformylation catalyzed by Tolman's [*N,N'*-bis(2,6-diisoproylphenyl)-2,6-pyridinedicarboxamido]-superoxo-copper(II) complex[31] may operate through a Baeyer-Villiger mechanism.[32] Under this hypothesis, shown in **Scheme 13**, aldehyde deformylation is enabled by increased α-C substitution due to the improved stabilization of a transient carbocation that is formed during the Criegee rearrangement step, where the α-C carbon migrates to the distal peroxy oxygen. Thus, the absence of deformylation products for substrates **B** and **C**, which both feature 2° α-C sites, suggests that these atoms possess insufficient carbocation stabilization that facilitates Criegee rearrangement during the Baeyer-Villiger mechanism. The absence of reactivity towards substrate **C** suggests that an α-H atom is required such that deprotonation in later steps of the Baeyer-Villiger mechanism to form the formic acid by-product. Indeed, even before the Baeyer-Villiger mechanism was posited, Watanebe *et al* recognized the need for an α-H atom's presence for deformylation to proceed.[24c]
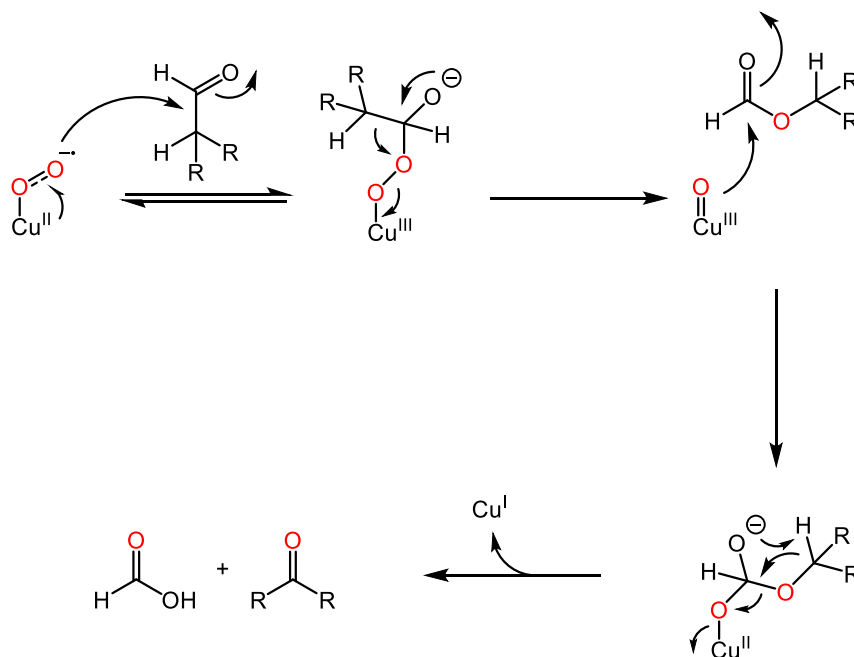
Scheme 13. Hypothesized metal-catalyzed Baeyer-Villiger oxidation mechanism.[32]

Alternatively, the P240$_{2B4}$ mechanism may be invoked for why catalytic deformylation of **A**, **B**, and **CCA** was not observed. In the absence of an external proton source, the aldehyde may not be reduced to an alkoxide when the M-O$_2$ adduct attacks the substrate to form the peroxo intermediate. However, this does not agree with the observation that **2-PPA** was selectively deformylated to acetophenone in the absence of a proton source; taken together, these results provide tentative evidence that the catalyst potentially operates through the Baeyer-Villiger mechanism rather than the P240$_{2B4}$ mechanism.

One of the highlights of the amidate ligand platform is the versatility for incorporating a variety of substituents that may influence the active site. Having identified a suitable substrate and established reactions conditions in the deformylation of **2-PPA**, the influence of steric and electronic factors of the deformylation was probed

using modified ligands L^{Me} and L^{CF3}. **$(Et_4N)_2[Co_2L_2{}^{CF3}]$** and **$(Et_4N)_2[Co_2L_2{}^{Me}]$** were both used to deformylate **2-PPA**, and the $-CF_3$ derivative showed virtually no capability of deformylation (see **Figure 5** in Experimental Section). The latter, on the other hand, showed consumption of substrate on par with **$(Et_4N)_2[Co_2L_2{}^{iPr}]$**. This provides early support for the notion that the active catalyst species features nucleophilic behavior, since it was predicted that the $-CF_3$ ligand substituent would shift electron density away from the M-O_2 adduct, thereby diminishing its nucleophilicity. The $-Me$ derivative, in contrast, would not be expected to significantly change the nucleophilicity in comparison to the $-^{i}Pr$ derivative since both are electron-donating groups. These results also highlight how the **H_3L^R** ligand platform shows increased depth of modularity over the TMC ligand platform, since our system allows insight into electronic effects, while the TMC ligand only allows insight into steric factors.
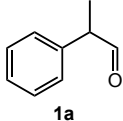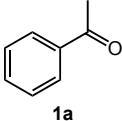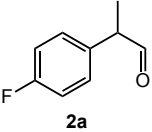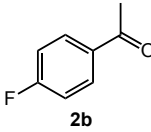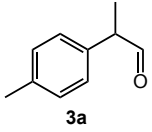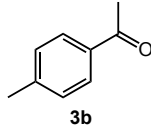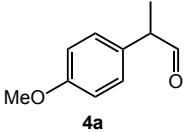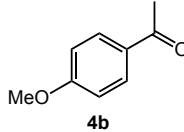
Entry	Substrate	Product	Yield
1	1a	1a	91.1%
2	2a	2b	*N.D.
3	3a	3b	40.0%
4	4a	4b	49.9%

Table 2. Aldehyde substrates tested for catalytic deformylation to investigate the influence of the *para*-substituents. *Reaction conditions:* In a typical procedure, 10 mol% of $(Et_4N)_2[Co_2L_2^{iPr}]$ and 1 mol. equivalent of substrate were dissolved in dry acetonitrile inside a glove box. The reaction mixture was then removed from the glove box and briefly evacuated of N_2 under a vacuum line. The reaction was then stirred for 24 hrs. under positive O_2 flow at 1 atm. The following day, the reaction mixture was concentrated *in vacuo*. The concentrate was then extracted with a 9:1 hexanes/EtOAc solution (3 x 5 mL), filtered through a plug of silica, and concentrated *in vacuo* for the isolated product. Yields are reported based upon isolable conversion of starting substrate.

After examining the influence of the ligand's **R** substituents on the rate of catalysis, we next decided to probe the deformylation mechanism $(Et_4N)_2[Co_2L_2^{iPr}]$ proceeds through by testing out a variety of **2-PPA** derivatives that feature varying steric

and electronic characteristics, as summarized in **Table 2**. Entries **2-4** were selected for the construction of a Hammett plot in future studies to better establish if nucleophilicity is a determining factor in deformylation by comparing kinetic rates of these substrates with cobalt catalysts supported by –Ph, -Me, and -CF$_3$ derivatives of **H$_3$L**. According to our hypothesis that the active mononuclear-superoxo species is nucleophilic in character, we predict that kinetic studies will reveal a slower k_{obs} for entries **3** and **4** due to the presence of electron-donating *para* substituents. In contrast, we predict entry **2** will possess a noticeably higher k_{obs} value due to the electron-withdrawing *para*-F substituent that would make the aldehyde C atom more electrophilic.
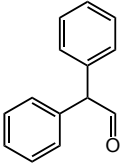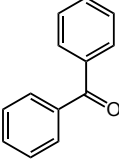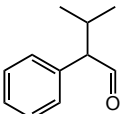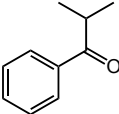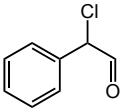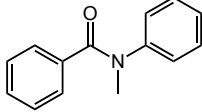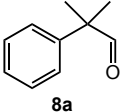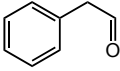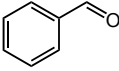
Entry	Substrate	Product	Yield
5	5a	5b	25.3%
6	6a	6b	49.9%
7	7a	*7b	N.D.
8	8a	----------------	N.R.
9	9a	9b	N.R.

Table 3. Aldehyde substrates tested for catalytic deformylation to investigate the influence of substituents on the α-C center. *Reaction conditions:* In a typical procedure, 10 mol% of catalyst and 1 mol. equivalent of substrate were dissolved in dry acetonitrile inside a glove box. The reaction mixture was then removed from the glove box and briefly evacuated of N_2 under a vacuum line. The reaction was then stirred for 24 hrs. under positive O_2 flow at 1 atm. The following day, the reaction mixture was concentrated *in vacuo*. The concentrate was then extracted with a 9:1 hexanes/EtOAc

solution (3 x 5 mL), filtered through a plug of silica, and concentrated *in vacuo* for the isolated product. Yields are reported based upon isolable conversion of starting substrate.

After reacting **(Et₄N)₂[Co₂L₂^{iPr}]** with a variety of *para*-substituted **2-PPA** derivatives, we then investigated the influence of substituents on the α-C center, as summarized in **Table 3**. **5** and **6** both showed fairly good conversion of substrate to product, yet isolated yields for **5** based on conversion of substrate was somewhat less than **2-4**'s, indicating potential difficulties in orienting the substrate with the active catalyst due to steric hindrance imposed by the bulkier α-C substituent. **7a** was selected in order to test if an electron-withdrawing group would influence reactivity. **7**'s GC-MS originally showed no peaks that would correlate with product **7b**. We conjectured that perhaps this was because the predicted benzoyl chloride product was too reactive and immediately decomposed under reaction conditions. In response, we repeated the reaction with triethylamine and N-methylaniline in order to intercept the unstable acyl chloride *in situ* and produce a more stable product, as shown in **Scheme 14**. GC-MS of this reaction produced a peak whose *m/z* agreed with the molecular mass of the predicted *N*-methyl-*N*-phenylbenzylamide product (**7b**), providing strong support that a benzoic chloride is indeed produced *in situ*. Attempts to scale up the reaction to attain a better yield for **7b** were unsuccessful, presumably due to further decomposition of **7b** during workup.
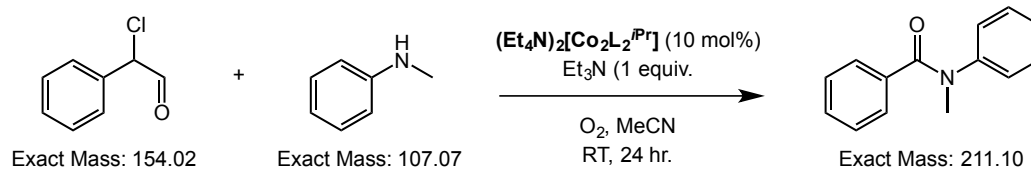
Scheme 14. Trapping experiment of potential benzoyl chloride product. Product identified by GC-MS.

Entry **8** only returned substrate, in agreement with Watanabe's predictions that an α-H atom must be present in order for deformylation to proceed.[24c] Importantly, **9** also only returned substrate instead of benzaldehyde as the expected product. This result suggests that in addition to a free α-H atom, the substrate must possess specifically a tertiary α-C atom for the reaction to successfully proceed.

We also attempted to synthesize a **2-PPA** derivative with a -CF₃ substituent on the α-C center via a previously reported procedure (depicted in **Scheme 15**) in the literature[33] in the hopes of investigating the influence of an electron-withdrawing α-C substituent whose mass was closer to **1a** than **7a**. Although the Wittig product was successfully made, repeated attempts at the acid-catalyzed hydrolysis of the olefin substrate to the aldehyde failed to yield product and only returned starting material. Future directions will involve varying the acid and the ratio of H_2O to acetone used to dissolve the olefin substrate.
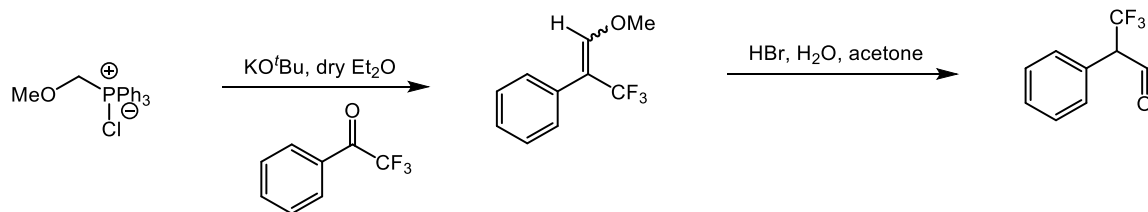
Scheme 15. Previously reported procedure for the synthesis of a -CF$_3$ α-substituted phenylacetaldehyde derivative.[33]

C. CONCLUSION

(Et$_4$N)$_2$[Co$_2$L$_2$^{iPr}] was shown to be catalytically active for the deformylation of **2-PPA** in the presence of O$_2$. Substituent variation on the ligand was employed and the observation that **(Et$_4$N)$_2$[Co$_2$L$_2$^{Me}]** also catalytically deformylates **2-PPA** to acetophenone while **(Et$_4$N)$_2$[Co$_2$L$_2$^{CF3}]** cannot support the hypothesis that the active catalytic M-O$_2$ species is likely of nucleophilic character. Attempts to deformylate **CCA** and several other aldehyde substrates that did not bear resemblance to **2-PPA**'s structure with **(Et$_4$N)$_2$[Co$_2$L$_2$^{iPr}]** showed no evidence of reactivity.

Efforts to probe the deformylation mechanism for additional insight into the nature of the active Co-O$_2$ adduct led us to test **(Et$_4$N)$_2$[Co$_2$L$_2$^{iPr}]**'s activity against a wide range of substrates based off of **2-PPA**. The results of these studies show that catalytic deformylation is only observed for substrates that include a tertiary α-C that also possesses an α-H atom. Furthermore, our results tentatively suggest that steric bulk at the α-C position impedes reactivity as evidenced by the comparatively low yield of entry **5** in **Table 3**.

Although reactions with a variety of **2-PPA** derivatives have now been established that they readily deformylate in the presence of $(Et_4N)_2[Co_2L_2{}^{iPr}]$, future experiments that repeat these reactions with $(Et_4N)_2[Co_2L_2{}^{R}]$, where **R** = -CF$_3$, Me, and Ph, must be run in order to further ascertain the nucleophilicity of the active species. We expect that kinetic studies comparing these catalysts will show a significant decrease in k_{obs} as **R** increasingly loses electron-donating ability. Likewise, we expect that kinetic studies comparing substrates **1a-4a** will show increasing k_{obs} as the *para* substituent gains electron density.

D. EXPERIMENTAL

General Information. All chemicals were obtained from Sigma-Aldrich of the highest purity available. Solvents were procured through a solvent purification system and then stored over 4 Å molecular sieves in the glove box. Aldehyde substrates were dried by stirring in anhydrous acetonitrile with 4 Å molecular sieves overnight under N$_2$ and then being distilled before bringing into the glove box. Ultra-high purity O$_2$ and N$_2$ were purchased from NexAir. Air-free reactions were run inside an Mbraun Labmaster 130 glove box. Product formation was studied via GC-MS with an Agilent Technologies 5977A Series GC/MSD System. NMR studies were conducted variously among a Varian Inova 400 MHz, VNMR 400 MHz, and a Mercury 300 MHz system.

Ligand Synthesis
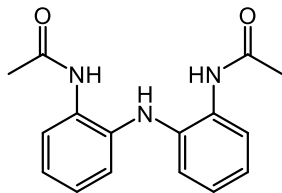
Preparation of HN(*o*-PhNHC(O)Me)₂ (H₃L^Me)

2.0 g (10.0376 mmol) of HN(*o*-PhNH₂)₂ was dissolved in 50 mL of anhydrous dichloromethane (DCM) under N₂ and cooled to 0 °C. 4.2 mL of triethylamine (3.0471 g, 30.11 mmol) was then added, followed by 1.8 mL of acetyl chloride (1.9872 g, 25.3179 mmol), which was pre-diluted in 10 mL of anhydrous DCM. The reaction mixture was left to warm to room temperature and stir overnight under a constant purge of N₂. The next day, the reaction mixture was extracted with saturated aqueous NaHCO₃ (3 x 30 mL) and brine (1 x 20 mL). The organic layer was dried with MgSO₄, filtered, and then concentrated by vacuum. The resulting concentrate was dissolved in minimal acetone and layered with diethyl ether to form the purified white powder product (2.33 g, 82%). ^{1}H NMR (δ, CDCl₃, 400 MHz): (ppm) 7.75 (s, 2H), 7.62 – 7.60 (d, 2 H), 7.11 – 7.07 (t, 2H), 7.03 – 6.99 (t, 2H), 6.92 – 6.90 (d, 2H), 5.67 (s, 1H), 2.15 (s, 6H). ^{13}C NMR (δ, CDCl₃, 400 MHz): (ppm) 169.47, 136.02, 128.69, 126.43, 124.48, 122.69, 120.70, 23.82. FTIR (KBR, cm^{-1}): ν(NH)$_{amine}$ 3385, ν(NH)$_{amide}$ 3266, ν(CO) 1648. ESI-MS: C₁₆H₁₈O₂N₃ m/z Calcd. 284.13935 Found 284.13906 [M+H]$^+$.

Complex Synthesis
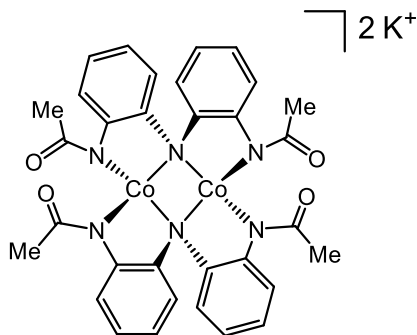
Preparation of K$_2$[Co$_2$L$_2$^{Me}]

Within a glove box, 82.10 (0.290 mmol) mg of H$_3$L^{Me} was dissolved in approximately 10 mL of dimethylformamide (DMF) to form a colorless solution. 43.31 mg (1.081 mmol) of potassium hydride was then added to this solution, turning yellow-brownish in color. Once gas evolution ceased, 62.96 mg (0.288 mmol) of cobalt bromide was added, and this reaction mixture was allowed to stir for an additional hour. The DMF was then evacuated, and the concentrate was re-dissolved in acetonitrile to crash out insoluble potassium bromide, which was filtered off through a medium porosity fritted filter. The acetonitrile solution was evacuated, and the concentrate was dissolved yet again in minimal acetonitrile this time. The reaction mixture was filtered through a pipette filter with Celite, and this solution was set for vapor diffusion crystallization with diethyl ether to form a few green X-ray quality crystals. FTIR (KBr, cm^{-1}): ν(CO) 1674. ^{1}H NMR (δ, CD$_3$CN, 400 MHz): (ppm) 58.39 (s), 27.52 (s), 8.56 (s), 5.45 (s), -104.74 (s).
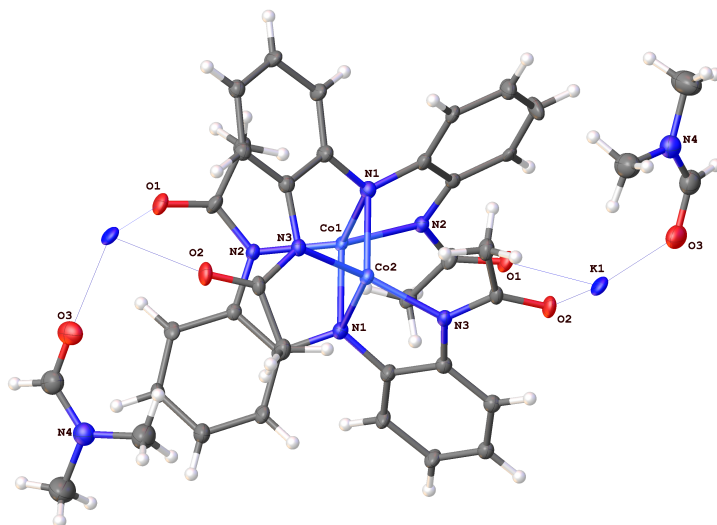
Figure 4. Crystallographic data of $K_2[Co_2L_2^{Me}]$.

Table 4. Crystallographic data of $K_2[Co_2L_2{}^{Me}]$.

Formula	$C_{22}H_{28}CoKN_5O_4$
$D_{calc.}$/ g cm^{-3}	1.468
m/mm^{-1}	0.937
Formula Weight	524.52
Colour	green
Shape	prism
Max Size/mm	0.34
Mid Size/mm	0.21
Min Size/mm	0.07
T/K	100(2)
Crystal System	orthorhombic
Space Group	Pbcn
a/Å	21.481(4)
b/Å	8.0245(14)
c/Å	27.541(5)
a/°	90
b/°	90
g/°	90
V/Å^3	4747.4(14)
Z	8
Z'	1

$Q_{min}/°$	1.479
$Q_{max}/°$	23.255
Measured Refl.	20537
Independent Refl.	3404
Reflections Used	1803
R_{int}	0.2382
Parameters	298
Restraints	260
Largest Peak	2.185
Deepest Hole	-1.308
GooF	1.226
wR_2 (all data)	0.3748
wR_2	0.2797
R_1 (all data)	0.2027
R_1	0.1215

Table 5. Bond Lengths in Å for $K_2[Co_2L_2{}^{Me}]$.

Atom	Atom	Length/Å
Co1	N1[1]	2.070(10)
Co1	N1	2.070(10)
Co1	N2	1.952(9)
Co1	N2[1]	1.952(9)
Co2	N1[1]	2.068(10)
Co2	N1	2.068(10)
Co2	N3[1]	1.943(9)
Co2	N3	1.943(9)
K1	O1[2]	2.737(8)
K1	O1	2.711(9)
K1	O2[1]	2.811(9)
K1	O2[3]	2.734(8)
K1	O3[4]	2.991(10)
K1	O3	2.775(9)
O1	K1[4]	2.738(8)
O1	C2	1.254(13)
O1SA	C3SA	1.22(2)
N1SA	C1SA	1.46(2)
N1SA	C2SA	1.46(2)
N1SA	C3SA	1.35(2)
O1SB	C3SB	1.22(2)

Atom	Atom	Length/Å
N1SB	C1SB	1.46(2)
N1SB	C2SB	1.47(2)
N1SB	C3SB	1.35(2)
O2	K1[5]	2.734(8)
O2	K1[1]	2.811(9)
O2	C15	1.245(12)
O3	K1[2]	2.991(10)
O3	C17	1.241(15)
N1	C8	1.430(15)
N1	C9	1.432(14)
N2	C2	1.352(14)
N2	C3	1.424(14)
N3	C14	1.432(15)
N3	C15	1.347(14)
N4	C17	1.341(16)
N4	C18	1.442(18)
N4	C19	1.422(17)
C1	C2	1.501(18)
C3	C4	1.427(15)
C3	C8	1.380(16)
C4	C5	1.430(17)
C5	C6	1.374(17)

Atom	Atom	Length/Å
C6	C7	1.388(17)
C7	C8	1.447(18)
C9	C10	1.374(17)
C9	C14	1.414(17)
C10	C11	1.421(16)
C11	C12	1.360(17)
C12	C13	1.399(16)
C13	C14	1.388(15)
C15	C16	1.510(16)

-------•

[1]1-X,+Y,1/2-Z;   [2]1/2-X,1/2+Y,+Z;   [3]-1/2+X,-1/2+Y,1/2-Z;   [4]1/2-X,-1/2+Y,+Z;

[5]1/2+X,1/2+Y,1/2-Z

Table 6. Bond Angles in ° for $K_2[Co_2L_2{}^{Me}]$.

Atom	Atom	Atom	Angle/°
N1[1]	Co1	N1	103.9(5)
N2[1]	Co1	N1[1]	84.8(4)
N2	Co1	N1[1]	110.8(4)
N2[1]	Co1	N1	110.8(4)
N2	Co1	N1	84.8(4)
N2[1]	Co1	N2	155.2(6)
N1[1]	Co2	N1	104.1(5)
N3	Co2	N1[1]	113.0(4)
N3[1]	Co2	N1[1]	84.7(4)
N3[1]	Co2	N1	113.0(4)
N3	Co2	N1	84.7(4)
N3	Co2	N3[1]	152.0(6)
O1	K1	O1[2]	141.1(3)
O1[2]	K1	O2[1]	75.9(2)
O1	K1	O2[1]	107.2(3)
O1	K1	O2[3]	77.6(2)
O1[2]	K1	O3	74.2(3)
O1[2]	K1	O3[4]	130.6(2)
O1	K1	O3[4]	71.2(2)
O1	K1	O3	144.3(3)

Atom	Atom	Atom	Angle/°
O2^3	K1	O1^2	82.3(2)
O2^3	K1	O2^1	149.9(3)
O2^3	K1	O3^4	68.9(2)
O2^3	K1	O3	122.4(3)
O2^1	K1	O3^4	141.1(2)
O3	K1	O2^1	71.1(3)
O3	K1	O3^4	88.1(3)
K1	O1	K1^4	95.7(2)
C2	O1	K1	131.3(8)
C2	O1	K1^4	133.0(8)
C1SA	N1SA	C2SA	116.5(15)
C3SA	N1SA	C1SA	119.4(15)
C3SA	N1SA	C2SA	124.0(16)
O1SA	C3SA	N1SA	122.5(13)
C1SB	N1SB	C2SB	116.5(16)
C3SB	N1SB	C1SB	119.4(15)
C3SB	N1SB	C2SB	124.0(16)
O1SB	C3SB	N1SB	122.5(13)
K1^5	O2	K1^1	93.5(2)
C15	O2	K1^1	126.5(8)
C15	O2	K1^5	139.8(8)
K1	O3	K1^2	88.8(3)

Atom	Atom	Atom	Angle/°
C17	O3	K1	124.8(9)
C17	O3	K1^2	142.2(9)
Co2	N1	Co1	76.0(3)
C8	N1	Co1	106.7(7)
C8	N1	Co2	121.0(7)
C8	N1	C9	117.3(10)
C9	N1	Co1	121.5(8)
C9	N1	Co2	108.4(7)
C2	N2	Co1	123.1(8)
C2	N2	C3	123.1(9)
C3	N2	Co1	111.9(7)
C14	N3	Co2	113.0(7)
C15	N3	Co2	121.9(7)
C15	N3	C14	123.2(9)
C17	N4	C18	120.2(12)
C17	N4	C19	123.5(12)
C19	N4	C18	115.8(11)
O1	C2	N2	125.8(11)
O1	C2	C1	118.8(10)
N2	C2	C1	115.3(9)
N2	C3	C4	122.1(10)
C8	C3	N2	116.7(10)

Atom	Atom	Atom	Angle/°
C8	C3	C4	121.0(11)
C3	C4	K1	98.0(7)
C3	C4	C5	118.2(11)
C5	C4	K1	109.1(8)
C6	C5	C4	121.8(12)
C5	C6	C7	119.0(12)
C6	C7	C8	121.7(11)
N1	C8	C7	122.8(10)
C3	C8	N1	118.9(11)
C3	C8	C7	118.3(10)
C10	C9	N1	123.2(11)
C10	C9	C14	119.5(11)
C14	C9	N1	117.2(10)
C9	C10	C11	121.0(12)
C12	C11	C10	118.6(12)
C11	C12	C13	121.4(11)
C14	C13	C12	120.1(11)
C9	C14	N3	116.2(10)
C13	C14	N3	124.4(11)
C13	C14	C9	119.3(11)
O2	C15	N3	126.8(11)
O2	C15	C16	119.0(10)

Atom	Atom	Atom	Angle/°
N3	C15	C16	114.2(9)
O3	C17	N4	122.5(14)

-------•

[1]1-X,+Y,1/2-Z;   [2]1/2-X,1/2+Y,+Z;   [3]-1/2+X,-1/2+Y,1/2-Z;   [4]1/2-X,-1/2+Y,+Z;

[5]1/2+X,1/2+Y,1/2-Z

Preparation of 1-(1-methoxyprop-1-en-2-yl)-4-methylbenzene
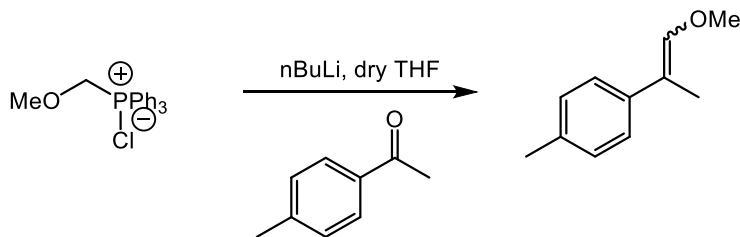
Product was prepared according to a modified procedure of the reported literature.[34] Under an inert N_2 atmosphere, 1.79 g (5.22 mmol) of (methoxymethyl)triphenylphosphonium chloride was dissolved in 100 mL of dry THF and cooled to -78 °C in a dry ice/acetone bath. 3.26 mL (0.334 g, 5.22 mmol) of 1.6 M nBuLi in hexanes was slowly syringed into the reaction mixture. The solution was allowed to stir for another 30 minutes at -78 °C before allowing it to warm up to room temperature, at which point it turned deep red in color. After 1 hour of stirring at room temperature, the solution was recooled to -78 °C, and 0.46 mL (0.464 g, 3.46 mmol) of 4'-methylacetophenone diluted in 1 mL of dry THF was added dropwise into the mixture. The reaction quickly turned yellow in color, and it was allowed to stir overnight at room temperature. The following day, the solution was dissolved in 80 mL of deionized water. The aqueous layer was extracted with Et_2O (2 x 50 mL), dried over $MgSO_4$, and concentrated *in vacuo* to yield a yellow oil. This oil was run through a column, first beginning with a 19:1 hexane/EtOAc mixture and gradually ending with a 9:1 hexane/EtOAc mixture. 27.9% yield. ^{1}H NMR (400 MHz, $CDCl_3$): δ (ppm) = 7.49 – 7.47 (d, 1H), 7.34 – 7.27 (m, 1 H), 7.20 – 7.08 (m, 2H), 6.35 (s, 0.5H), 6.07 (s, 1H), 3.70

– 3.69 (m, 1.5H), 3.65 – 3.64 (m, 1.5H), 2.34 – 2.31 (m, 3H), 1.97 – 1.96 (m, 1.5H), 1.90

– 1.88 (m, 1.5H). Spectrum matches that of previously reported literature.

Preparation of 2-(*p*-tolyl)propanal
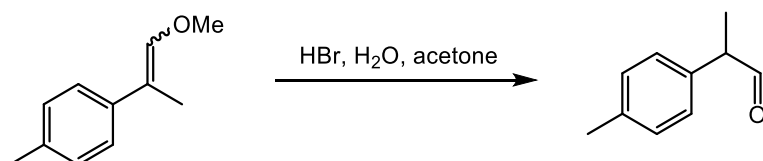
Product was prepared according to a modified procedure of the reported literature.[34]

156.4 mg (0.965 mmol) of the starting material was dissolved in 2 mL of acetone and 0.5

mL of deionized water and cooled to 0 °C. 0.1 mL of a 48% HBr solution was then

syringed into this mixture. The solution was stirred for 2 days at room temperature.

Then, the solution was neutralized with aqueous $NaHCO_3$. The aqueous solution was

extracted with Et_2O (3 x 5 mL), dried with $MgSO_4$, filtered, and concentrated *in vacuo*

for the product. 65.7% yield. ^{1}H NMR (400 MHz, $CDCl_3$): δ (ppm) = 9.66 (s, 1H), 7.69

– 7.44 (m, 2H), 7.21 – 7.09 (m, 2H), 3.50 – 3.45 (q, 1H), 2.35 (s, 3H), 1.43 – 1.41 (d,

3H). Spectrum matches that of previously reported literature.

Preparation of 2-chloro-2-phenylacetaldehyde
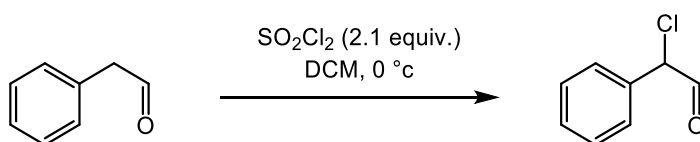
Product was prepared according to a modified procedure of the reported literature.[35] 5 mL (5.40 g, 44.9 mmol) of phenylacetaldehyde was diluted in 50 mL of DCM and cooled to 0 °C. 7.62 mL (12.74 g, 94.37 mmol) of sulfuryl chloride was then syringed dropwise into the reaction mixture, and the solution was left to stir overnight. The next day, the product was extracted with aqueous $NaHCO_3$ (3 x 30 mL), dried with $MgSO_4$, filtered, and concentrated *in vacuo* for an oil product. 17.0% yield. ^1H NMR (400 MHz, $CDCl_3$): δ (ppm) = 9.53 (d, 0.5H), 9.52 (d, 0.5H), 7.47 − 7.34 (m, 5 H), 5.21 − 5.20 (d, 1H). Spectrum matches that of previously reported literature.
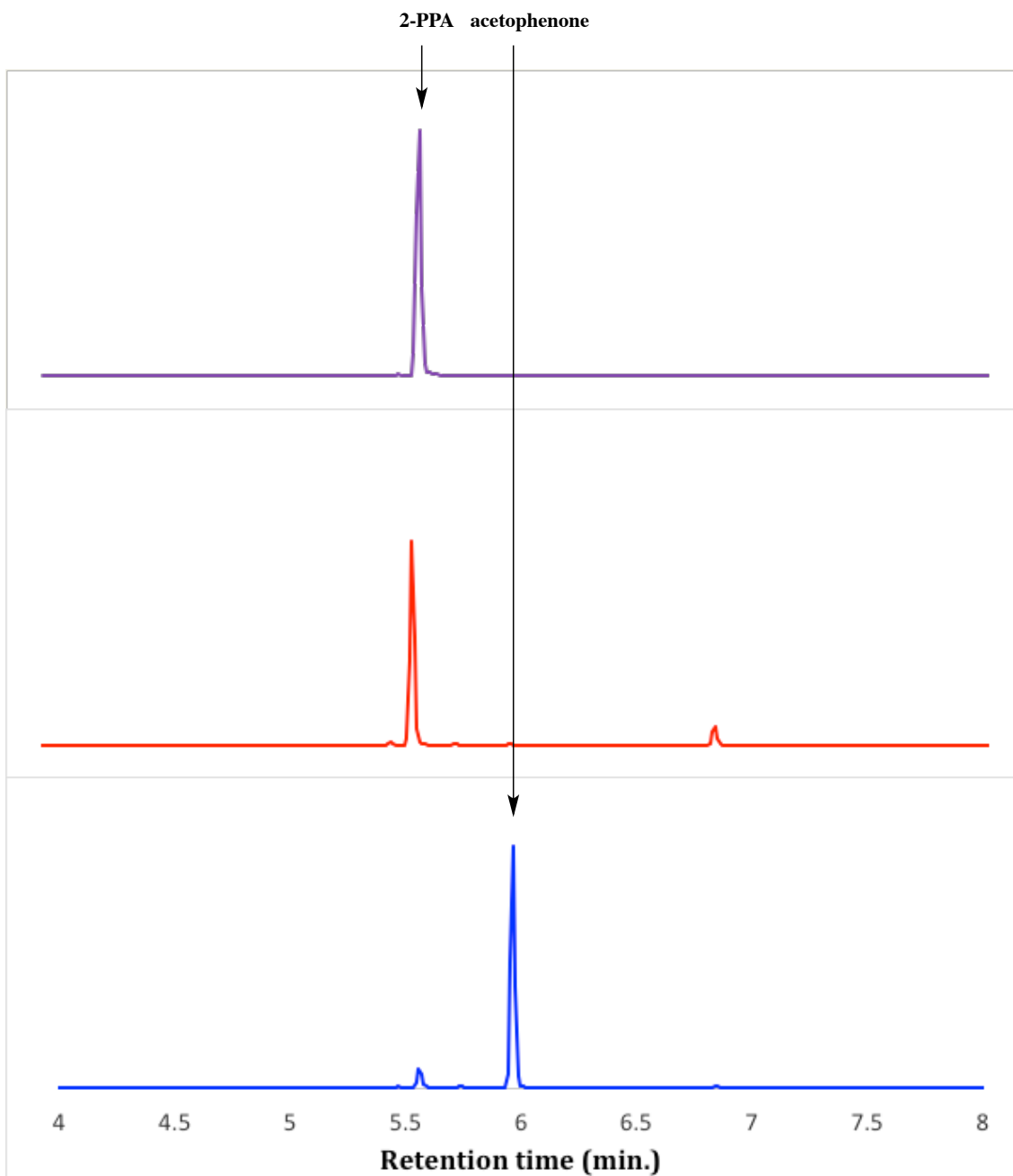
Figure 5. GC-MS chromatograms of 2-PPA deformylation with various catalysts. Top: **(Et₄N)₂[Co₂L₂ᵢᴾʳ]**, middle: **(Et₄N)₂[Co₂L₂ᴹᵉ]**, bottom: **(Et₄N)₂[Co₂L₂ᶜᶠ³]**. *Reaction conditions:* In a typical procedure, 10 mol% of catalyst and 1 mol. equivalent of substrate were dissolved in dry acetonitrile inside a glove box. The reaction mixture was then removed from the glove box and briefly evacuated of N₂ under a vacuum line. The

reaction was then stirred for 24 hrs. under positive O_2 flow at 1 atm. The following day, an aliquot was removed from the reaction mixture, diluted in excess dichloromethane and then filtered through a plug of silica. The solution was then submitted for GC-MS analysis.
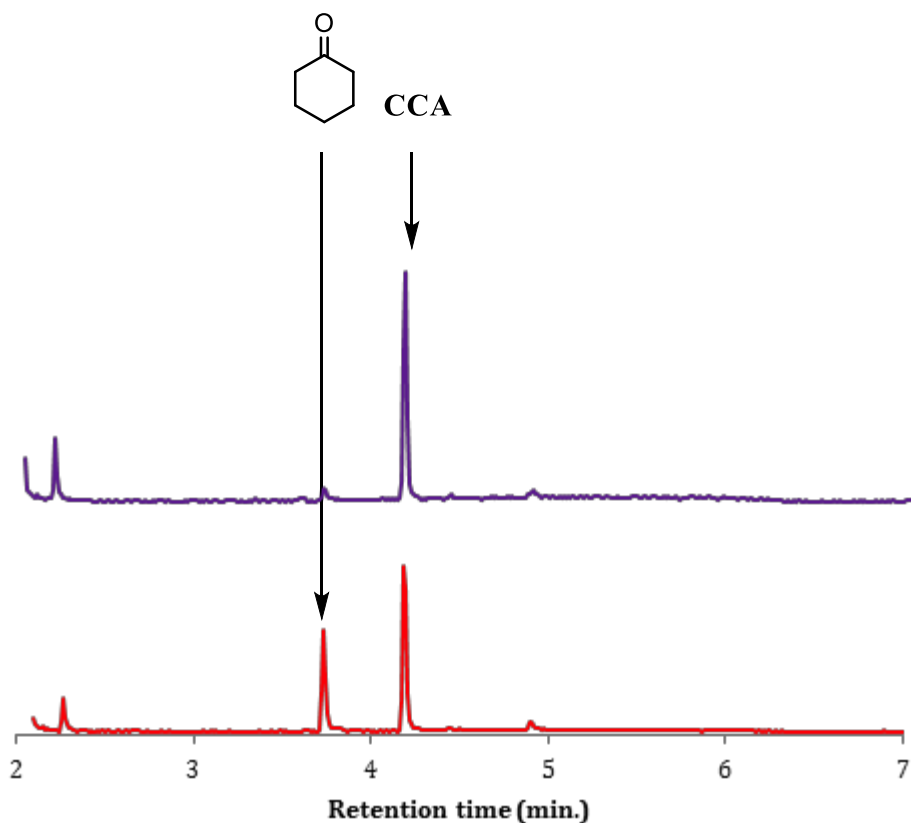
Figure 6. CCA deformylation at various solvent and temperature conditions with 10 mol% $(Et_4N)_2[Co_2L_2{}^{iPr}]$ under a constant purge of O_2 at 1 atm. Top: MeCN, 0 °C. Bottom: MeCN, 70 °C. *Reaction conditions:* In a typical procedure, 10 mol% of $(Et_4N)_2[Co_2L_2{}^{iPr}]$ and 1 mol. equivalent of substrate were dissolved in dry acetonitrile inside a glove box. The reaction mixture was then removed from the glove box and briefly evacuated of N_2 under a vacuum line. The reaction was then stirred for 24 hrs. under positive O_2 flow at 1 atm. The following day, an aliquot was removed from the

reaction mixture, diluted in excess dichloromethane and then filtered through a plug of silica. The solution was then submitted for GC-MS analysis.

Deformylation of 1a
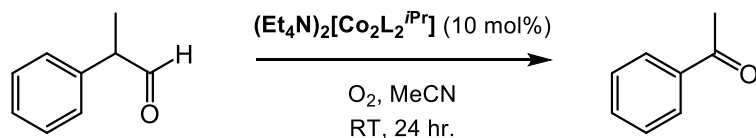
Within a glove box, 58.8 mg (0.0560 mmol) of $(Et_4N)_2[Co_2L_2{}^{iPr}]$ was dissolved in 60 mL of MeCN to produce a green solution. 0.15 mL (150.3 mg, 1.12 mmol) of pure **1a** was syringed into the reaction mixture. This reaction mixture was removed from the glove box and briefly evacuated of N_2 under a vacuum line. The reaction mixture was then placed under positive O_2 pressure at 1 atm, quickly becoming very dark purple, and stirred in this state overnight at room temperature. The following day, the reaction mixture was evacuated to concentration. The concentrate was extracted with a 9:1 hexane/ethyl acetate solution (3 x 5 mL). This was passed through a plug of silica for a pale yellow solution. This was evacuated to concentrate, yielding 122 mg (1.02 mmol) of **1b** (91.1% yield). ^{1}H NMR (400 MHz, CDCl$_3$): δ (ppm) = 7.99 – 7.95 (m, 2H), 7.60 – 7.54 (m, 1H), 7.50 - 7.43 (m, 2H), 2.61 (s, 3H). Spectrum matches that of previously reported literature.[36]

Deformylation of 2a
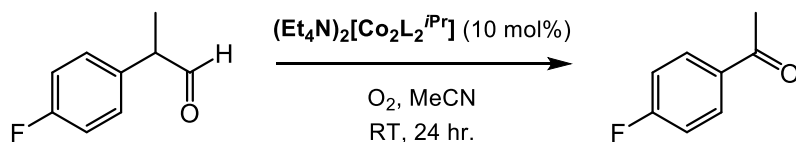
Within a glove box, 16.2 mg (0.0154 mmol) of $(Et_4N)_2[Co_2L_2{}^{iPr}]$ was dissolved in 15 mL of MeCN to produce a green solution. A 0.01903 mM stock solution of **2a** was prepared by diluting 94.1 mg (0.619 mmol) of pure **2a** in 10 mL of MeCN in a 10 mL volumetric flask for a 0.619 mM solution. 1 mL was taken from this and diluted to 10 mL of MeCN again for a 0.0619 mM solution, and then 3.08 mL was syringed from this and diluted up to 10 mL of MeCN again for the final 0.01903 mM solution. 7.00 mL (20.3 mg, 0.133 mmol) of this stock solution was syringed into the reaction mixture. This reaction mixture was removed from the glove box and briefly evacuated of N_2 under a vacuum line. The reaction mixture was then placed under positive O_2 pressure at 1 atm, quickly becoming very dark purple, and stirred in this state overnight at room temperature. The following day, the reaction mixture was evacuated to concentration. The concentrate was extracted with a 9:1 hexane/ethyl acetate solution (3 x 5 mL). This was passed through a plug of silica for a pale yellow solution. This was evacuated to concentrate, yielding 1.1 mg (0.80% yield) of **2b**. There was likely decomposition of either the product or the starting material, which resulted in the minimal isolable yield. Because not enough material could be gathered for ^1H NMR, the product was submitted for GC-MS. The product peak is located at 5.450 min. GC-MS $m/z = 138.1$.

Deformylation of 3a
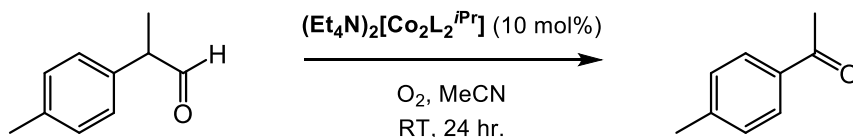
Within a glove box, 17.0 mg (0.0162 mmol) of $(Et_4N)_2[Co_2L_2{}^{iPr}]$ was dissolved in 15 mL of MeCN to produce a green solution. A 0.02536 mM stock solution of **3a** was prepared by diluting 93.9 mg (0.634 mmol) of pure **3a** to 25 mL of MeCN in a volumetric flask. 6.90 mL (25.9 mg, 0.175 mmol) of this stock solution was syringed into the reaction mixture. This reaction mixture was removed from the glove box and briefly evacuated of N_2 under a vacuum line. The reaction mixture was then placed under positive O_2 pressure at 1 atm, quickly becoming very dark purple, and stirred in this state overnight at room temperature. The following day, the reaction mixture was evacuated to concentration. The concentrate was extracted with a 9:1 hexane/ethyl acetate solution (3 x 5 mL). This was passed through a plug of silica for a pale yellow solution. This was evacuated to concentrate, yielding 9.4 mg (0.070 mmol) of **3b** (40.0% yield). ^{1}H NMR (400 MHz, CDCl$_3$): δ (ppm) = 7.68 – 7.62 (m, 2H), 7.53 – 7.51 (m, 1H), 7.47 – 7.42 (m, 2H), 2.57 (s, 3H), 2.40 (s, 3H). Spectrum matches that of previously reported literature.[37]
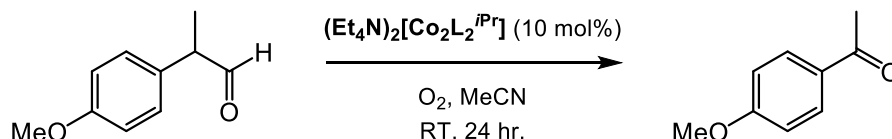
Deformylation of 4a

Within a glove box, 27.4 mg (0.026 mmol) of $(Et_4N)_2[Co_2L_2{}^{iPr}]$ was dissolved in 15 mL of MeCN to produce a green solution. A 0.07186 mM stock solution of **4a** was prepared

by diluting 117.9 mg (0.7186 mmol) of pure **4a** to 10 mL of MeCN in a volumetric flask.

3.97 mL (46.9 mg, 0.286 mmol) of this stock solution was syringed into the reaction

mixture. This reaction mixture was removed from the glove box and briefly evacuated of

N_2 under a vacuum line. The reaction mixture was then placed under positive O_2

pressure at 1 atm, quickly becoming very dark purple, and stirred in this state overnight at

room temperature. The following day, the reaction mixture was evacuated to

concentration. The concentrate was extracted with a 9:1 hexane/ethyl acetate solution (3

x 5 mL). This was passed through a plug of silica for a pale yellow solution. This was

evacuated to concentrate, yielding 21.4 mg (0.143 mmol) of **4b** (49.9% yield). ^{1}H NMR

(400 MHz, CDCl$_3$): δ (ppm) = 7.95 – 7.93 (d, 2H), 6.94 – 6.92 (d, 2H), 3.89 (s, 3H), 2.55

(s, 3H). Spectrum matches that of previously reported literature.[38]

Deformylation of 5a
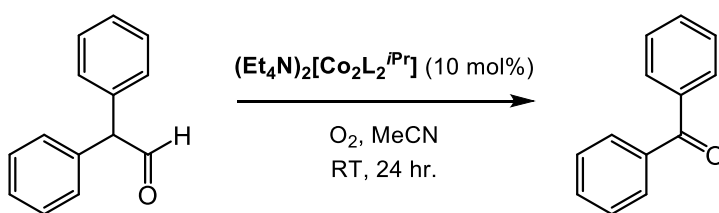
Within a glove box, 100.5 mg (0.09567 mmol) of (Et$_4$N)$_2$[Co$_2$L$_2{}^{iPr}$] was dissolved in 50

mL of MeCN to produce a green solution. A 0.19038 mM stock solution of **5a** was

prepared by diluting 0.68 mL (747.2 mg, 3.808 mmol) of pure **5a** to 20 mL of MeCN in a

volumetric flask. 5.0 mL (187 mg, 0.952 mmol) of this stock solution was syringed into

the reaction mixture. This reaction mixture was removed from the glove box and briefly

evacuated of N_2 under a vacuum line. The reaction mixture was then placed under

positive O_2 pressure at 1 atm, quickly becoming very dark purple, and stirred in this state

overnight at room temperature. The following day, the reaction mixture was evacuated to

concentration. The concentrate was extracted with a 9:1 hexane/ethyl acetate solution (3

x 5 mL). This was passed through a plug of silica for a pale yellow solution. This was

evacuated to concentrate, yielding 44.0 mg (0.241 mmol) of **5b** (25.3% yield). ^{1}H NMR

(400 MHz, CDCl$_3$): δ (ppm) = 7.81 – 7.78 (m, 4H), 7.60 – 7.56 (m, 2H), 7.50 – 7.5 (m,

4H). Spectrum matches that of previously reported literature.[36]

Deformylation of 6a

Within a glove box, 19.2 mg (0.0183 mmol) of $(Et_4N)_2[Co_2L_2{}^{iPr}]$ was dissolved in 10 mL

of MeCN to produce a green solution. A 0.02192 mM stock solution of **6a** was prepared

by diluting 88.9 mg (0.546 mmol) of pure **6a** to 25 mL of MeCN in a volumetric flask.

8.9 mL (31.6 mg, 0.195 mmol) of this stock solution was syringed into the reaction

mixture. This reaction mixture was removed from the glove box and briefly evacuated of

N_2 under a vacuum line. The reaction mixture was then placed under positive O_2

pressure at 1 atm and stirred in this state overnight at room temperature. The following

day, the reaction mixture was evacuated to concentration. The concentrate was extracted

with a 9:1 hexane/ethyl acetate solution (3 x 5 mL), which was then passed through a

plug of silica. This solution was then evacuated to concentration to yield 14.4 mg (0.097

mmol) of product (49.9% yield). ^{1}H NMR (400 MHz, CDCl$_3$): δ (ppm) = 7.96 – 7.93 (m,

2H), 7.55 – 7.16 (m, 3H), 3.60 – 3.50 (tt, 1H), 1.21 – 1.20 (d, 6H). Spectrum matches that of previously reported literature.[39]
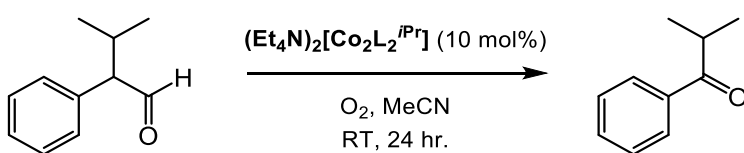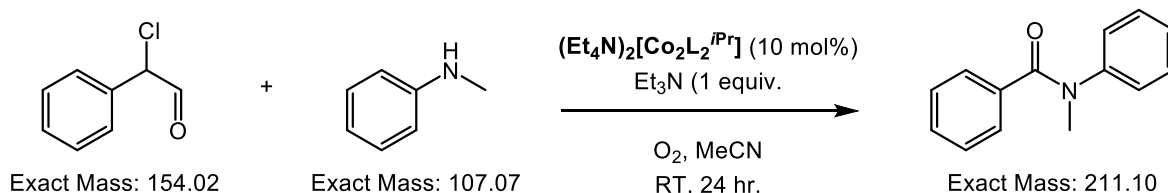
Deformylation of 7a

Within a glove box, 12.9 mg (0.0123 mmol) of $(Et_4N)_2[Co_2L_2{}^{iPr}]$ was dissolved in 10 mL of MeCN to produce a green solution. A 0.09519 mM stock solution of **7a** was prepared by diluting 293 mg (1.902 mmol) of pure **9a** to 20 mL of MeCN in a volumetric flask. 1.0 mL of this stock solution was syringed into the reaction mixture. 0.01 mL of freshly distilled Et_3N and 0.01 mL of freshly distilled N-methylaniline were added to the reaction mixture, yielding a turquoise-colored solution. This reaction mixture was removed from the glove box and briefly evacuated of N_2 under a vacuum line. The reaction mixture was then placed under positive O_2 pressure at 1 atm and stirred in this state overnight at room temperature. The following day, the now brown-colored reaction mixture was evacuated to concentration. The concentrate was extracted with a 9:1 hexane/ethyl acetate solution (3 x 5 mL). This was passed through a plug of silica for a bright orange solution, with green precipitate suspended on top of the silica. This bright orange solution was submitted to GC-MS analysis for identification of **7b**. Product peak was located at 12.249 min. GC-MS $m/z = 211.10$.

Deformylation of 8a and 9a

Within a glove box, approximately 10 mg (0.0095 mmoL) of $(Et_4N)_2[Co_2L_2{}^{iPr}]$ was dissolved in 10 mL of MeCN to produce a green solution. A 0.19038 mM stock solution of substrate was prepared by diluting 0.42 mL of pure substrate to 20 mL of MeCN in a 20 mL volumetric flask. 0.5 mL of this stock solution was syringed into the reaction mixture. This reaction mixture was removed from the glove box and briefly evacuated of N_2 under a vacuum line. The reaction mixture was then placed under positive O_2 pressure at 1 atm, quickly becoming very dark purple, and stirred in this state overnight at room temperature. The following day, a 2 mL aliquot of the reaction mixture was diluted in excess DCM to crash out the catalyst. This mixture was then passed through a plug of silica and submitted to GC-MS analysis for identification of product. GC-MS showed no peaks indicative of reactivity for both **8a** and **9a** and only returned peaks correlating to the substrates for both entries.

III. Aerobic Alcohol Oxidation to Ketones and Aldehydes Catalyzed by $(PPh_4)_2[Cu_2L_2{}^{iPr}]$

A. INTRODUCTION

The oxidation of alcohol substrates to selectively produce ketones or aldehydes is a ubiquitous transformation that is often accomplished through the use of stoichiometric manganese- and chromium-based oxidants, such as $KMnO_4$ and pyridinium chlorochromate (PCC).[1] Few examples exist of first-row transition metal catalysts capable of oxidizing alcohols to carbonyls relative to more well-established Ru[40] and Pd catalysts.[41] Oxides of molybdenum are commonly used to regioselectively and catalytically oxidize secondary alcohols in the presence of primary alcohols.[42] Unfortunately, these catalysts also require hydrogen peroxide in stoichiometric equivalents as the oxidant. Fewer examples, still, exist of first-row transition metal-mediated alcohol oxidation that utilize O_2 as the terminal oxidant. One of the earliest cases of such a catalyst system comes from Riviére and coworkers' report on the aerobic oxidation of benzylic alcohols with copper-amine complexes.[43] However, their system required two molar equivalents of copper for every equivalent of substrate.

The field of aerobic oxidation of alcohols with first-row transition metals further advanced with a seminal report by Markó and Urch on the use of di-substituted azo compounds as co-catalysts to the copper-amine complexes reported earlier by Riviére *et al.*[44] Markó found that di-substituted azo compounds such as di-*tert*-butylazodicarboxylate (DBAD) greatly enhanced the lifetime and turnover activity of the catalyst, as well as the reaction rate. Along with Markó's discovery of the Cu/DBAD system, many examples of superior performing Cu-nitroxyl or Cu-TEMPO systems have also been reported which, after extensive mechanistic studies, have been found to operate through 1 e$^-$ transfers from both the Cu and TEMPO to achieve the net 2 e$^-$ transfer necessary for alcohol oxidation (**Figure 7**).[45]
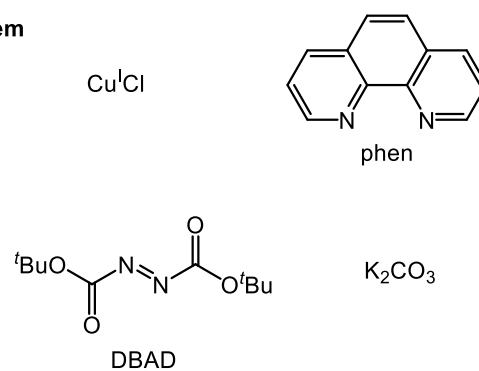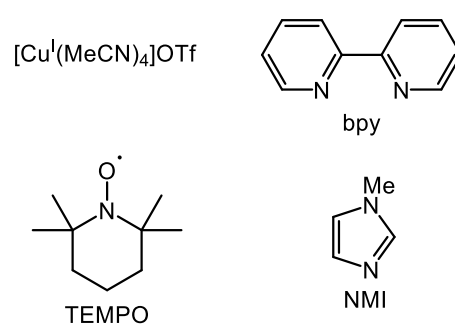
Figure 7. Comparison of Cu/DBAD and Cu/TEMPO components for aerobic oxidation of alcohol.[46]

It was early on hypothesized that the Cu/DBAD catalyst system operated through a similar mechanism as the Cu/nitroxyl catalyst systems. In both cases, a six-membered intermediate is posited to lead to a hydride transfer from the copper-alkoxide species to yield the final oxidized product, as shown in **Scheme 16**.
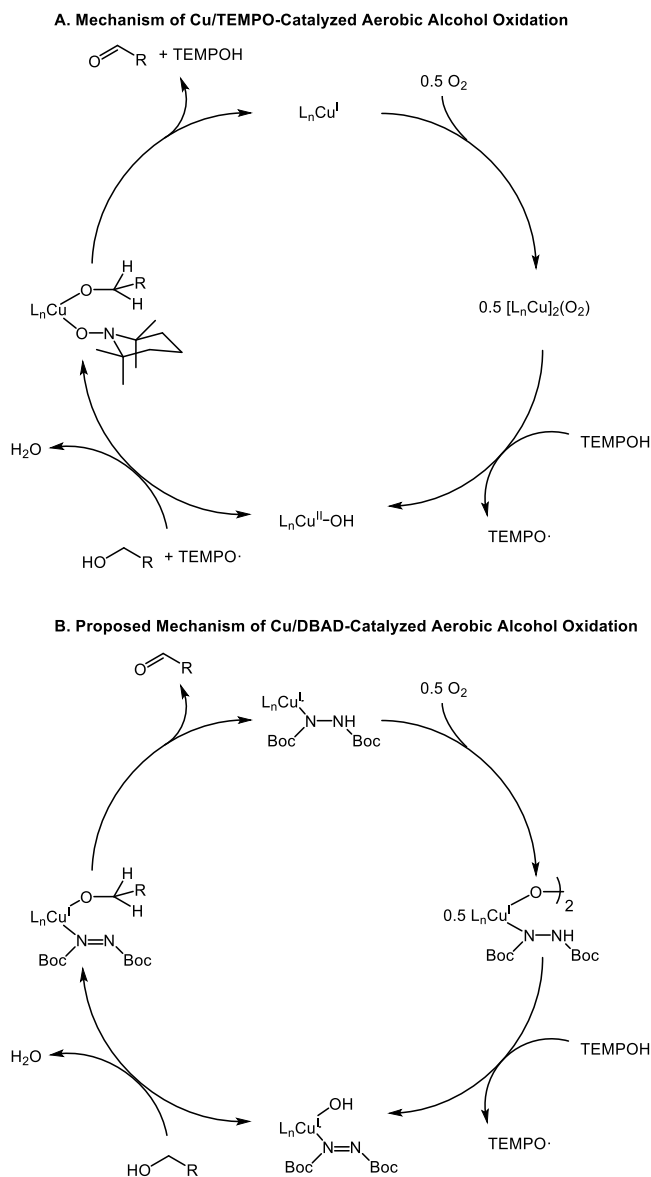
Scheme 16. A) Mechanism of Cu/TEMPO catalyzed aerobic alcohol oxidation. **B)** Proposed mechanism of Cu/DBAD-catalyzed aerobic alcohol oxidation.[46]
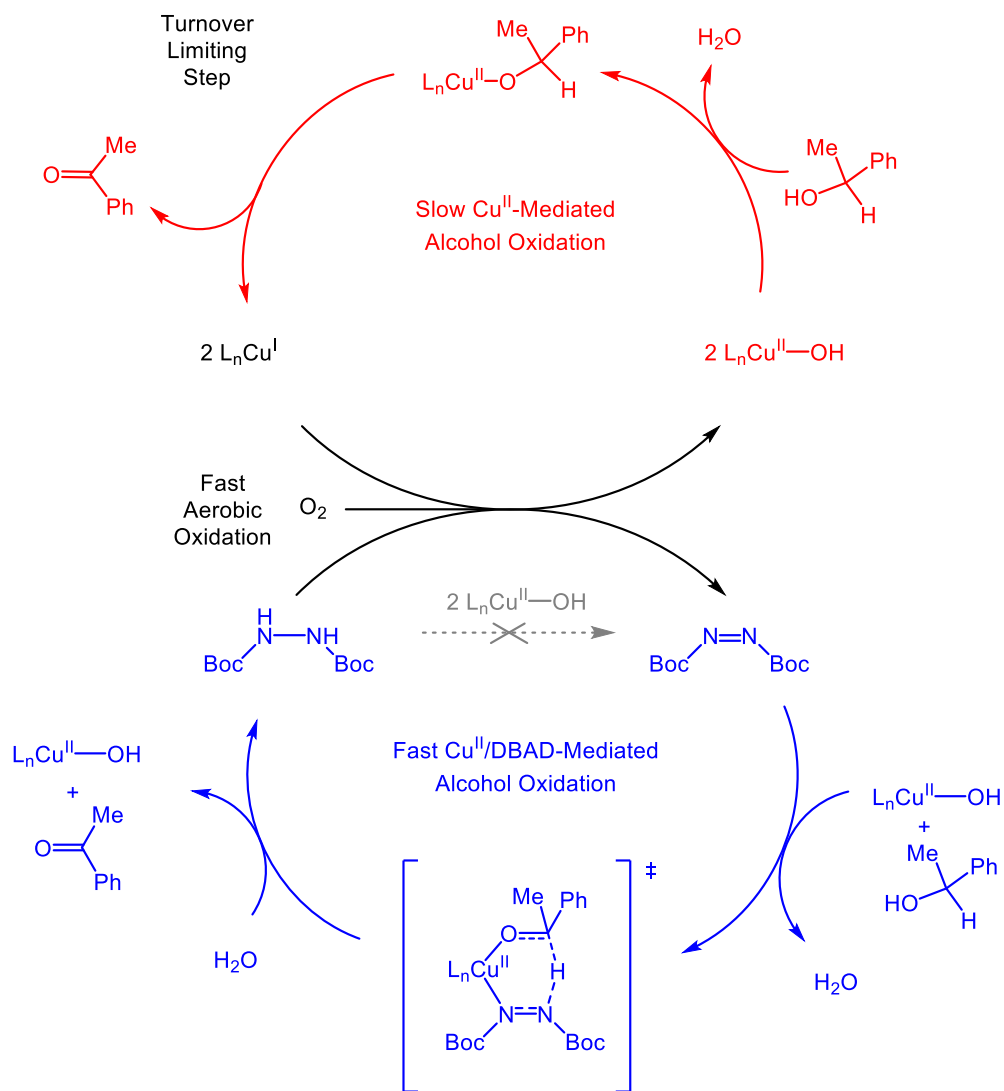
Scheme 17. Revised mechanism proposed by Stahl *et al* on Cu/DBAD catalyzed aerobic oxidation of alcohols.[46] The mechanism differs greatly from the original proposed mechanism by Markó and features two interdependent but poorly cooperative catalytic cycles.

A recent report by McMann and Stahl argues against this shared mechanism with an elegant series of kinetic studies that revealed, among other facts, 1) a kinetic burst at the beginning of the reaction that was not pO_2-dependent, and 2) Cu^{II} and $DBADH_2$ as

the catalytic resting state.[46] Stahl's revised mechanism, as shown in **Scheme 17**, proposes two interdependent catalytic cycles, composed of a slow Cu^{II}-only mediated alcohol oxidation and a faster Cu^{II}/DBAD-mediated oxidation. According to this mechanism, the reason the Cu/DBAD system performs less efficiently than the Cu/TEMPO system for alcohol oxidation is that Cu^{II} and DBAD exhibit poor redox cooperativity with one another. In the Cu/TEMPO case, the Cu^{II} and TEMPO co-catalysts oxidize the alcohol substrate by one electron each to form Cu^I and TEMPO-H, respectively. These two species are then oxidized by one equivalent of O_2 to regenerate the catalytic cycle anew. In contrast, Cu^{II} behaves as a Lewis acid towards the DBAD and alkoxide intermediate in the Cu/DBAD system. The key rate-determining step for the fast bottom cycle is the formation of the $DBAD-H_2$ species, which must be oxidized by Cu^{II} in order for the entire catalytic cycle to continue. However, Cu^{II} is not an effective oxidant for $DBAD-H_2$, and so both Cu^{II} and $DBAD-H_2$ accumulate in their resting states. Cu^I would be a better oxidant for $DBAD-H_2$, yet Cu^I forms in the slower Cu^{II}-only mediated cycle, whereas for the Cu/TEMPO system, Cu^I is a natural by-product of the reaction mechanism. These results provide important insight for future iterations of catalyst design that would remedy the lack of redox cooperativity between the metal and organic co-catalysts.

Based off of Stahl's analysis of the Cu/DBAD system, we were inspired to investigate if our oxygen-activating catalyst scaffold is also capable of aerobically oxidizing alcohols to ketones and aldehydes when co-catalyzed by DBAD. We were motivated not only by the possibility of identifying other organic substrates our catalyst platform is suitable for oxidizing, but also by Stahl's critical insight that redox

cooperativity is the main reason the Cu/DBAD catalyst system performs less effectively than the Cu/TEMPO system. We hypothesized that if our catalyst is capable of the aerobic oxidation of alcohols to ketones and aldehydes, then that altering **H₃L**'s R substituent would also provide an avenue for improving the redox cooperativity between our catalyst and DBAD. This second portion of this thesis will detail efforts on applying our catalyst to this class of reaction.

B. RESULTS AND DISCUSSION

We started our investigations with the conversion of 1-phenylethanol to acetophenone as the model reaction. Preliminary experiments at room temperature with both **(Et₄N)₂[Co₂L₂^{iPr}]** and DBAD yielded a small amount of acetophenone as product in the GC-MS chromatogram. We believed it was worth repeating the reaction with **(PPh₄)₂[Cu₂L₂^{iPr}]**, because we speculated that the cobalt and copper centers of the two catalysts bind to O₂ in different manners (**Figure 8**)[47], which would potentially unlock different reactivity profiles.
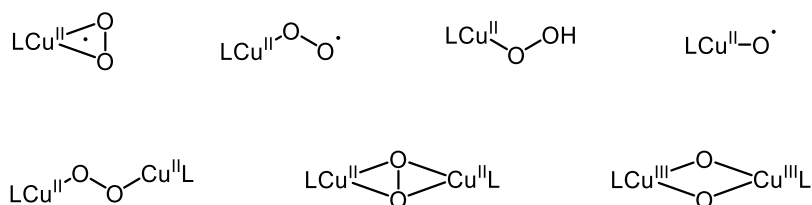
Figure 8. Different possible binding modes of copper with O₂.[47]

Indeed, preliminary GC-MS experiments with **(PPh₄)₂[Cu₂L₂^{iPr}]** at the same conditions that **(Et₄N)₂[Co₂L₂^{iPr}]** was used to oxidize 1-phenylethanol qualitatively appeared to produce slightly more product. Further control reactions that omitted either

(PPh₄)₂[Cu₂L₂^{iPr}] or DBAD revealed that no product formation is observed without the presence of DBAD, while only a negligible amount of product formation is observed without the presence of **(PPh₄)₂[Cu₂L₂^{iPr}]** (see **Figure 11** in Experimentals). This established that although DBAD serves as an oxidant, it is an ineffective reagent for alcohol oxidation, while **(PPh₄)₂[Cu₂L₂^{iPr}]** by itself cannot oxidize 1-phenylethanol to acetophenone without an organic co-catalyst.

Based on Markó's original report which ran the reaction at 70-90 °C, we attempted to increase catalytic turnover by increasing the temperature from 25 °C to 40-50 °C. To our delight, the GC-MS chromatograms of the reaction mixtures demonstrated much higher product yields at elevated temperatures. Furthermore, a comparison of the copper-catalyzed and cobalt-catalyzed reaction chromatograms indicate that **(Et₄N)₂[Co₂L₂^{iPr}]** demonstrates less product selectivity and turnover than **(PPh₄)₂[Cu₂L₂^{iPr}]** (see **Figure 9** in Experimental section), thus providing support for our earlier speculations that the two catalysts feature different reactivity patterns due to potentially different binding modes with O_2. Further attempts at optimization by lowering catalyst loading of **(PPh₄)₂[Cu₂L₂^{iPr}]** unfortunately showed reduced product formation, and so we optimized the conditions with 10 mol% catalyst loading for all follow-up reactions. The optimized reaction conditions are summarized in **Scheme 18**.
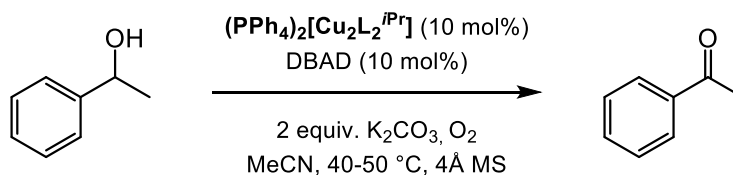
Scheme 18. Model reaction with 1-phenylethanol catalytically oxidized to acetophenone. GC-MS indicated over 80% conversion of the substrate to product (see **Figure 9** in

Experimental section), yet isolated yield characterized by ^{1}H NMR was 44% (see **Table 7**), presumably due to loss of product during work-up.

Following these optimizations, additional substrates first tested by Markó in his report were tested as summarized in **Table 7**.[44] Neither **2** nor **5** provided evidence of isomerization of the C-C double bonds, yet integration of **5**'s ^{1}H NMR of the product mixture reveals a near 1-to-4 mixture of **5a** and **5b**, potentially indicating lower product formation with aliphatic alcohols. However, this is more likely due to accidental excess loading of **5a** into the reaction mixture, thus leading to less product yield. **3** demonstrates that the alcohol oxidation is unaffected by electron-withdrawing groups on the aryl functionality. Finally, reaction **4** only yields oxidation products at the alcohol terminus, with no oxidation of the thiomethyl end, indicating excellent chemoselectivity of **(PPh$_4$)$_2$[Cu$_2$L$_2$^{iPr}]** towards hydroxyl groups over other functional groups.

Entry	Substrate	Product	Yield	Time (hr.)
1	OH 1a	O 1b	43.7%	24
2	2a	2b	71.9%	48
3	Cl 3a	Cl 3b	59.7%	48
4	S 4a	S 4b	64.6%	48
5	5a	5b	*50%	24

Table 7. List of alcohol substrates tested for catalytic aerobic oxidation by **(PPh$_4$)$_2$[Cu$_2$L$_2$^{iPr}]**. *Reaction conditions*: In a typical procedure, 10 mol% of catalyst, 10 mol% of DBAD, 1 mol. equivalent of alcohol, 2 mol. equivalent of K$_2$CO$_3$, and 4 Å MS were dissolved in dry acetonitrile inside a glove box. The reaction mixture was then removed from the glove box and briefly evacuated of N$_2$ under a vacuum line. The reaction was then stirred at 40 – 50 °C for 24 h under positive O$_2$ flow at 1 atm. The following day, the 4 Å MS was filtered off. The filtrate was then concentrated *in vacuo* and then extracted with a 9:1 hexanes/EtOAc solution (3 x 5 mL), filtered through a plug of silica, and concentrated *in vacuo* again for the isolated product. Yields are reported based upon starting alcohol substrate.

C. CONCLUSIONS

(PPh$_4$)$_2$[Cu$_2$L$_2$^{iPr}] was found to exhibit a similar level of substrate tolerance and product selectivity and formation for the oxidation of alcohols to ketones and aldehydes

as the DBAD co-catalyzed copper-amine complex system first reported by Markó and coworkers. Furthermore, repeating the same alcohol oxidation reactions with $(Et_4N)_2[Co_2L_2{}^{iPr}]$ revealed much lower product formation and selectivity in comparison to the copper analogue, providing potential justification for our predictions that the copper and cobalt metal centers bind with O_2 in different modes and consequently exhibit different reactivity profiles.

In order to probe this reactivity more, further optimizations may be made to this reaction. Markó's original report found that the reaction ran more efficiently in a relatively non-polar solvent such as benzene.[44] For the purposes of our investigations, though, we opted for the more polar acetonitrile because it better solvates $(PPh_4)_2[Cu_2L_2{}^{iPr}]$. We have not yet tested if the reaction rate increases in a solvent system such as a 4:1 mixture of toluene and DMF, which would also avail the possibility of further increasing the temperature, thereby further increasing the reaction rate.

Much more interesting than experiments that optimize the solvent and temperature conditions, however, are experiments investigating different organic co-catalysts and variations of H_3L. Stahl and coworkers' conclusion that DBAD and Cu share poor redox cooperativity obviously implies that improved iterations on the DBAD/Cu system should seek to rectify this issue. As suggested by Stahl, this may take the form of modified $(phen)Cu^{II/I}$ redox couples or different azo co-catalysts.[46]

Although we cannot conclude based off of our current compiled data if $(PPh_4)_2[Cu_2L_2{}^{iPr}]$ operates through either the Cu/TEMPO mechanism or Stahl's revised Cu/DBAD mechanism, the role of redox cooperativity is central to both mechanisms. The fact that our ligand platform H_3L^R features access to a wide range of redox potentials

by simply altering the **R** group suggests we may be able to improve the redox cooperativity between the copper center and the DBAD co-catalyst by identifying the proper **R** substituent.

D. EXPERIMENTAL
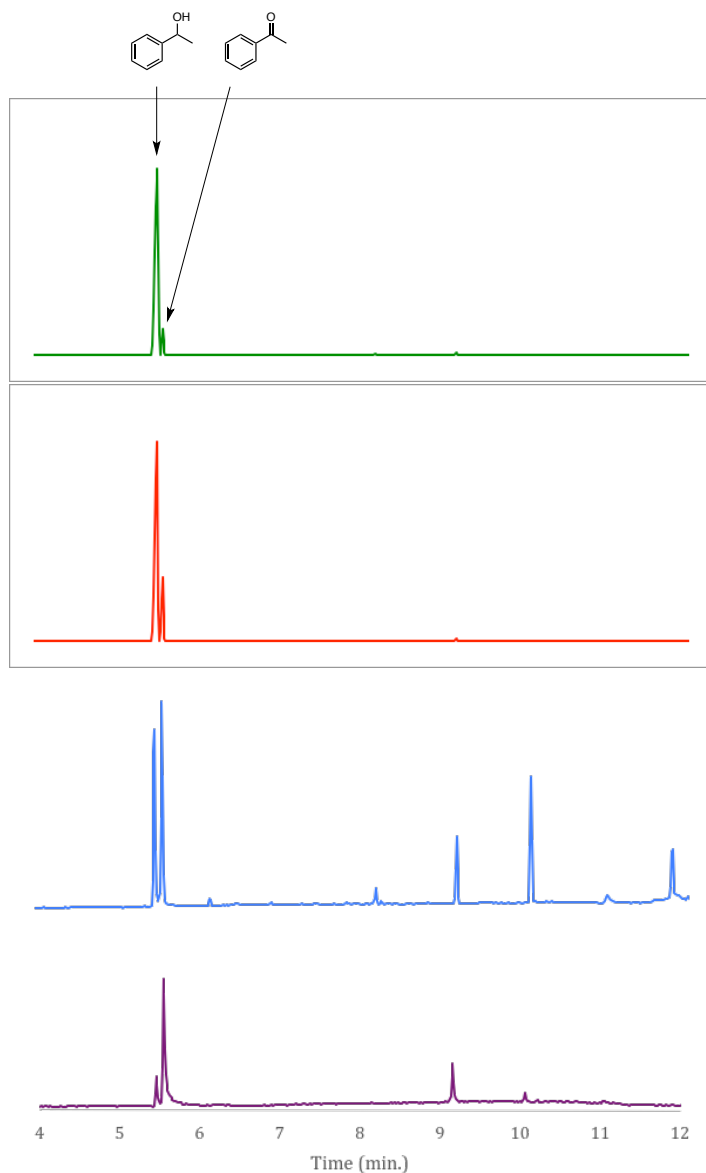
Figure 9. GC-MS of alcohol oxidation reactions under various temperatures and various catalysts. *Reaction conditions*: 10 mol% loading of DBAD and cat., 1 mol. equivalent of 1-phenyethanol, 2 mol. equivalent of K_2CO_3, and 4 Å MS were dissolved in dry acetonitrile. Green: **(Et$_4$N)$_2$[Co$_2$L$_2$^{iPr}]** at RT. Red: **(PPh$_4$)$_2$[Cu$_2$L$_2$^{iPr}]** at RT. Blue: **(Et$_4$N)$_2$[Co$_2$L$_2$^{iPr}]** at 40-50 °C. Purple: **(PPh$_4$)$_2$[Cu$_2$L$_2$^{iPr}]** at 40-50 °C.
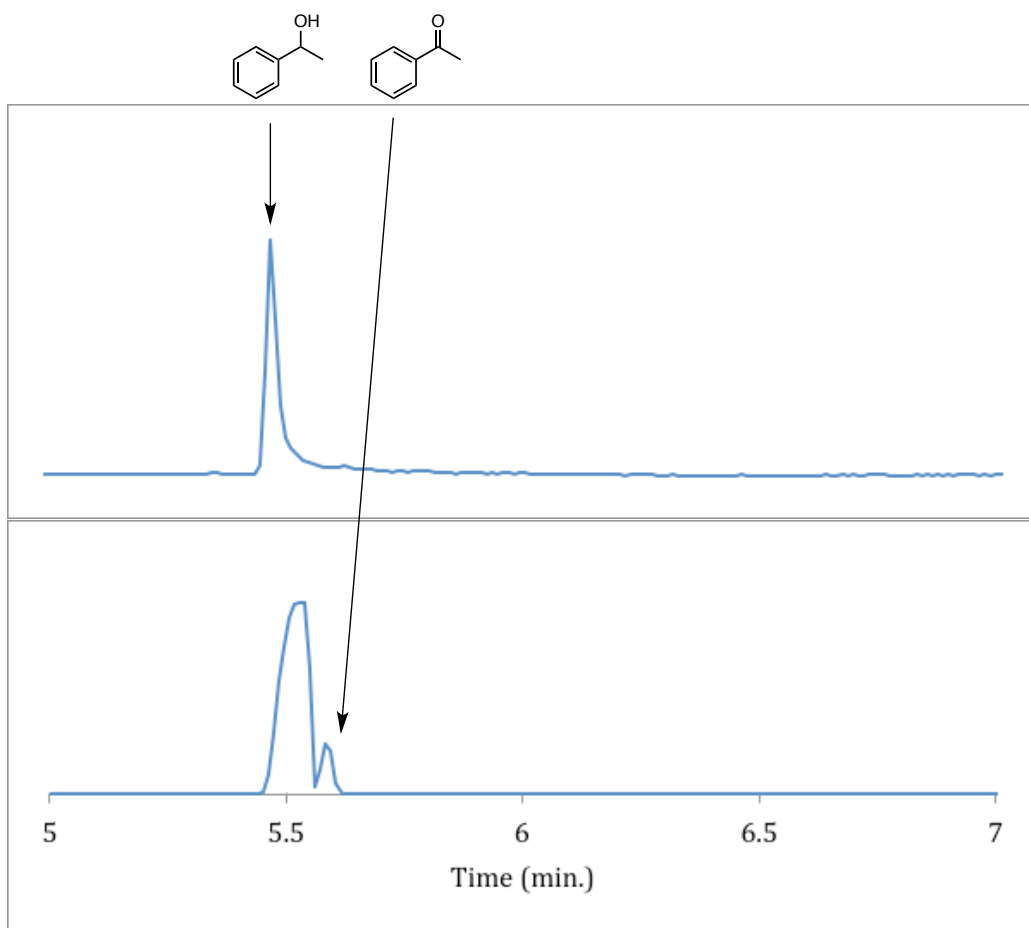
Figure 10. GC-MS of control reactions for alcohol oxidation comparing absence of either DBAD or **(PPh₄)₂[Cu₂L₂^{iPr}]**. *Reaction conditions*: 10 mol% loading of DBAD and **(PPh₄)₂[Cu₂L₂^{iPr}]**, 1 mol. equivalent of 1-phenyethanol, 2 mol. equivalent of K₂CO₃, and 4 Å MS were dissolved in dry acetonitrile. Top: Without DBAD but with **(PPh₄)₂[Cu₂L₂^{iPr}]**. Bottom: With DBAD but without **(PPh₄)₂[Cu₂L₂^{iPr}]**.

Oxidation of 1a
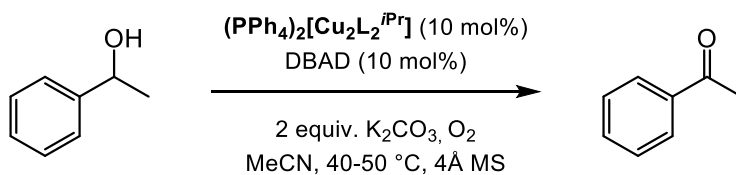
Within a glove box, 119.0 mg (0.0806 mmol) of $(PPh_4)_2[Cu_2L_2{}^{iPr}]$ was mixed in with 26.0 mg (0.113 mmol) of DBAD, 225.8 mg (1.634 mmol) of K_2CO_3, 0.10 mL (102.0 mg, 0.836 mmol) of pure **1a**, and 4 Å MS in 20 mL of MeCN to form a dark purple solution. This reaction mixture was removed from the glove box and briefly evacuated of N_2 under a vacuum line. The reaction mixture was then heated to 50 °C and stirred for 2 days under a constant stream of O_2 at 1 atm. The mixture was then filtered through a medium porosity frit to remove the 4 Å MS. The filtrate was collected and evacuated to concentration, then extracted with a 9:1 hexanes/EtOAc solution (3 x 5 mL). This was then passed through a plug of silica and evacuated to concentration again to yield 43.9 mg (0.365 mmol) of product (43.7% yield). ^{1}H NMR (400 MHz, CDCl$_3$): δ (ppm) = 7.98 − 7.95 (m, 2H), 7.59 − 7.55 (m, 1H), 7.49 − 7.44 (m, 2H), 2.61 (s, 3H). Spectrum matches that of reported literature.[36]

Oxidation of 2a

$(PPh_4)_2[Cu_2L_2{}^{iPr}]$ (10 mol%)
DBAD (10 mol%)

2 equiv. K_2CO_3, O_2
MeCN, 40-50 °C, 4Å MS
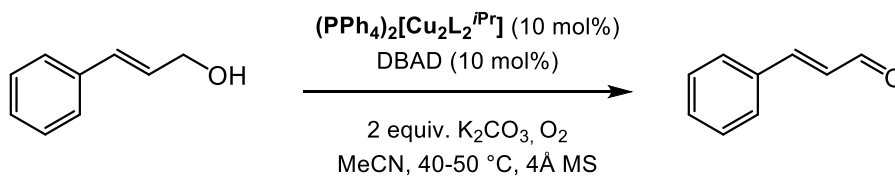
Within a glove box, 25.5 mg (0.0173 mmol) of $(PPh_4)_2[Cu_2L_2{}^{iPr}]$ was mixed in with 8.9 mg (0.039 mmol) of DBAD, 120.9 mg (0.8748 mmol) of K_2CO_3, 27.2 mg (0.203 mmol) of **2a**, and 4 Å MS in 20 mL of MeCN to form a dark purple solution. This reaction mixture was removed from the glove box and briefly evacuated of N_2 under a vacuum line. The reaction mixture was then heated to 50 °C and stirred for 2 days under a constant stream of O_2 at 1 atm. The mixture was then filtered through a medium porosity

frit to remove the 4 Å MS. The filtrate was collected and evacuated to concentration, then extracted with a 9:1 hexanes/EtOAc solution (3 x 5 mL). This was then passed through a plug of silica and evacuated to concentration again to yield 19.3 mg (0.146 mmol) of product (71.9% yield). ^{1}H NMR (400 MHz, CDCl$_3$): δ (ppm) = 9.72 – 9.63 (d, 1H), 7.57 – 7.54 (m, 2H), 7.45 – 7.41 (m, 3H), 6.74 – 6.67 (q, 2H). Spectrum matches that of reported literature.[48]

Oxidation of 3a
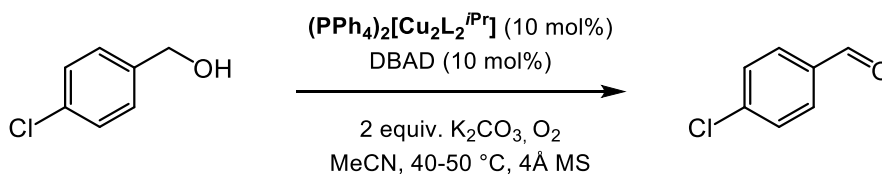
Within a glove box, 25.8 mg (0.0175 mmol) of (PPh$_4$)$_2$[Cu$_2$L$_2{}^{iPr}$] was mixed in with 5.6 mg (0.024 mmol) of DBAD, 93.3 mg (0.675 mmol) of K$_2$CO$_3$, 33.0 mg (0.231 mmol) of **3a**, and 4 Å MS in 20 mL of MeCN to form a dark purple solution. This reaction mixture was removed from the glove box and briefly evacuated of N$_2$ under a vacuum line. The reaction mixture was then heated to 50 °C and stirred for 2 days under a constant stream of O$_2$ at 1 atm. The mixture was then filtered through a medium porosity frit to remove the 4 Å MS. The filtrate was collected and evacuated to concentration, then extracted with a 9:1 hexanes/EtOAc solution (3 x 5 mL). This was then passed through a plug of silica and evacuated to concentration again to yield 19.3 mg (0.138 mmol) of product (59.7% yield). ^{1}H NMR (400 MHz, CDCl$_3$): δ (ppm) = 9.97 (d, 1H), 7.82 – 7.80 (d, 2H), 7.51 – 7.49 (d, 2H). Spectrum matches that of reported literature.[36]

Oxidation of 4a

Within a glove box, 31.0 mg (0.021 mmol) of $(PPh_4)_2[Cu_2L_2{}^{iPr}]$ was mixed in with 11.7 mg (0.051 mmol) of DBAD, 75.0 mg (0.543 mmol) of K_2CO_3, 34.5 mg (0.224 mmol) of **4a**, and 4 Å MS in 20 mL of MeCN to form a dark purple solution. This reaction mixture was removed from the glove box and briefly evacuated of N_2 under a vacuum line. The reaction mixture was then heated to 50 °C and stirred for 2 days under a constant stream of O_2 at 1 atm. The mixture 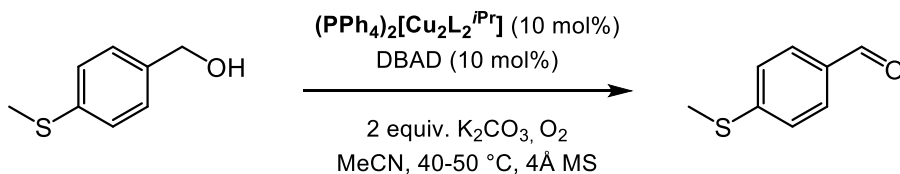was then filtered through a medium porosity frit to remove the 4 Å MS. The filtrate was collected and evacuated to concentration, then extracted with a 9:1 hexanes/EtOAc solution (3 x 5 mL). This was then passed through a plug of silica and evacuated to concentration again to yield 22.0 mg (0.145 mmol) of product (64.6% yield). ^1H NMR (400 MHz, $CDCl_3$): δ (ppm) = 9.90 (s, 1H), 7.76-7.74 (d, 2H), 7.31 – 7.29 (d, 2H), 2.51 (s, 3H). Spectrum matches that of reported literature.[49]

Oxidation of 5a
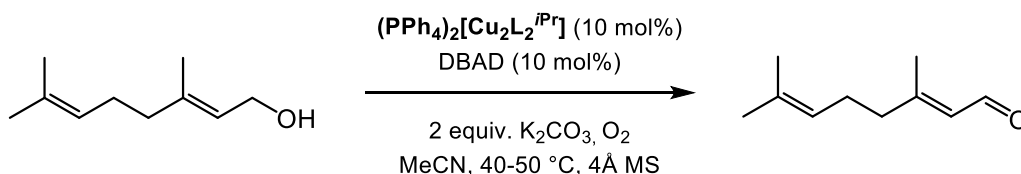
Within a glove box, 29.2 mg (0.020 mmol) of $(PPh_4)_2[Cu_2L_2{}^{iPr}]$ was mixed in with 6.8 mg (0.030 mmol) of DBAD, 72.1 mg (0.522 mmol) of K_2CO_3, 0.04 mL (35.6 mg, 0.231 mmol) of **5a**, and 4 Å MS in 20 mL of MeCN to form a dark purple solution. This

reaction mixture was removed from the glove box and briefly evacuated of N_2 under a vacuum line. The reaction mixture was then heated to 50 °C and stirred for 2 days under a constant stream of O_2 at 1 atm. The mixture was then filtered through a medium porosity frit to remove the 4 Å MS. The filtrate was collected and evacuated to concentration, then extracted with a 9:1 hexanes/EtOAc solution (3 x 5 mL). This was then passed through a plug of silica and evacuated to concentration. 68.8 mg (0.452 mmol) of product was isolated, indicating that the 0.04 mL of **5a** was inaccurately measured out. Integration of the ^{1}H NMR produces a rough estimate of 25% yield. This is calculated by comparing the aldehyde H peak of **5b** to the hydroxyl H peak of **5a**. ^{1}H NMR (400 MHz, CDCl$_3$): δ (ppm) = 9.95 – 9.93 (d, 1H), 5.89 – 5.86 (d, 1H), 5.43 – 5.39 (t, 1H), 1.70 (s, 3H), 1.25 (s, 6H), 2.23 – 2.21 (m, 1H), 0.88 – 0.85 (t, 2H). Spectrum matches that of reported literature.[50]

IV. REFERENCES

1.   Delaude, L.; Laszlo, P., A Novel Oxidizing Reagent Based on Potassium Ferrate(VI)1. *The Journal of Organic Chemistry* **1996,** *61* (18), 6360-6370.

2.   Carey, J. S.; Laffan, D.; Thomson, C.; Williams, M. T., Analysis of the reactions used for the preparation of drug candidate molecules. *Organic & Biomolecular Chemistry* **2006,** *4* (12), 2337-2347.

3.   (a) Punniyamurthy, T.; Velusamy, S.; Iqbal, J., Recent Advances in Transition Metal Catalyzed Oxidation of Organic Substrates with Molecular Oxygen. *Chemical Reviews* **2005,** *105* (6), 2329-2364; (b) Gunasekaran, N., Aerobic Oxidation Catalysis with Air or Molecular Oxygen and Ionic Liquids. *Advanced Synthesis & Catalysis* **2015,** *357* (9), 1990-2010; (c) Schultz, M. J.; Sigman, M. S., Recent advances in homogeneous transition metal-catalyzed aerobic alcohol oxidations. *Tetrahedron* **2006,** *62* (35), 8227-8241.

4.   Emile, L. T. Process for the production of ethylene oxide. 1935.

5.   Smidt, J.; Hafner, W.; Jira, R.; Sieber, R.; Sedlmeier, J.; Sabel, A., The Oxidation of Olefins with Palladium Chloride Catalysts. *Angewandte Chemie International Edition in English* **1962,** *1* (2), 80-88.

6.   Chirik, P. J.; Wieghardt, K., Radical Ligands Confer Nobility on Base-Metal Catalysts. *Science* **2010,** *327* (5967), 794-795.

7.   Wachter, R. M.; Montague-Smith, M. P.; Branchaud, B. P., β-Haloethanol Substrates as Probes for Radical Mechanisms for Galactose Oxidase. *Journal of the American Chemical Society* **1997,** *119* (33), 7743-7749.

8.   Jørgensen, C. K., Differences between the four halide ligands, and discussion remarks on trigonal-bipyramidal complexes, on oxidation states, and on diagonal elements of one-electron energy. *Coordination Chemistry Reviews* **1966,** *1* (1), 164-178.

9.   Eisenberg, R.; Gray, H. B., Noninnocence in Metal Complexes: A Dithiolene Dawn. *Inorganic chemistry* **2011,** *50* (20), 9741-9751.

10.   Marsh, E. N.; Waugh, M. W., Aldehyde Decarbonylases: Enigmatic Enzymes of Hydrocarbon Biosynthesis. *ACS catalysis* **2013,** *3* (11).

11.   (a) Woggon, W.-D., Cytochrome P450: Significance, reaction mechanisms and active site analogues. In *Bioorganic Chemistry: Models and Applications*, Schmidtchen, F. P., Ed. Springer Berlin Heidelberg: Berlin, Heidelberg, 1997; pp 39-96; (b) Groves, J. T., Models and Mechanisms of Cytochrome P450 Action. In *Cytochrome P450: Structure, Mechanism, and Biochemistry*, Ortiz de Montellano, P. R., Ed. Springer US: Boston, MA, 2005; pp 1-43.

12.   Li, N.; Norgaard, H.; Warui, D. M.; Booker, S. J.; Krebs, C.; Bollinger, J. M., *J. Am. Chem. Soc.* **2011,** *133*, 7148.

13.   Meunier, B.; de Visser, S. P.; Shaik, S., *Chem. Rev.* **2004,** *104*, 3947.

14.   Bernard, A.; Joubes, J., Arabidopsis cuticular waxes: advances in synthesis, export and regulation. *Progress in lipid research* **2013,** *52* (1), 110-29.

15.   Howard, R. W.; Blomquist, G. J., *Annu. Rev. Entymol.* **2005,** *50*, 371.

16.   Dennis, M. W.; Kolattukudy, P. E., *Arch. Biochem. Biophys.* **1991,** *287*, 268.

17.   Thompson, E. A.; Siiteri, P. K., Utilization of Oxygen and Reduced Nicotinamide Adenine Dinucleotide Phosphate by Human Placental Microsomes during Aromatization of Androstenedione. *Journal of Biological Chemistry* **1974,** *249* (17), 5364-5372.

18.   Ohno, K.; Tsuji, J., Organic synthesis by means of noble metal compounds. XXXV. Novel decarbonylation reactions of aldehydes and acyl halides using rhodium complexes. *Journal of the American Chemical Society* **1968,** *90* (1), 99-107.

19.   Doughty, D. H.; Pignolet, L. H., Catalytic decarbonylation of aldehydes. *Journal of the American Chemical Society* **1978,** *100* (22), 7083-7085.

20.   Kreis, M.; Palmelund, A.; Bunch, L.; Madsen, R., A General and Convenient Method for the Rhodium-Catalyzed Decarbonylation of Aldehydes. *Advanced Synthesis & Catalysis* **2006,** *348* (15), 2148-2154.

21.   Fristrup, P.; Kreis, M.; Palmelund, A.; Norrby, P.-O.; Madsen, R., The Mechanism for the Rhodium-Catalyzed Decarbonylation of Aldehydes: A Combined Experimental and Theoretical Study. *Journal of the American Chemical Society* **2008,** *130* (15), 5206-5215.

22.   Murphy, S. K.; Park, J.-W.; Cruz, F. A.; Dong, V. M., Rh-catalyzed C–C bond cleavage by transfer hydroformylation. *Science* **2015,** *347* (6217), 56-60.

23.   (a) McCandlish, E.; Miksztal, A. R.; Nappa, M.; Sprenger, A. Q.; Valentine, J. S.; Stong, J. D.; Spiro, T. G., Reactions of superoxide with iron porphyrins in aprotic solvents. A high spin ferric porphyrin peroxo complex. *Journal of the American Chemical Society* **1980,** *102* (12), 4268-4271; (b) Schappacher, M.; Weiss, R.; Montiel-Montoya, R.; Trautwein, A.; Tabard, A., Formation of an iron(IV)-oxo "picket-fence" porphyrin derivative via reduction of the ferrous dioxygen adduct and reaction with carbon dioxide. *Journal of the American Chemical Society* **1985,** *107* (12), 3736-3738; (c) Groves, J. T.; Watanabe, Y., Oxygen activation by metalloporphyrins related to

peroxidase and cytochrome P-450. Direct observation of the oxygen-oxygen bond cleavage step. *Journal of the American Chemical Society* **1986,** *108* (24), 7834-7836.

24.   (a) Wertz, D. L.; Sisemore, M. F.; Selke, M.; Driscoll, J.; Valentine, J. S., Mimicking Cytochrome P-450 2B4 and Aromatase: Aromatization of a Substrate Analogue by a Peroxo Fe(III) Porphyrin Complex. *Journal of the American Chemical Society* **1998,** *120* (21), 5331-5332; (b) Selke, M.; Valentine, J. S., Switching on the Nucleophilic Reactivity of a Ferric Porphyrin Peroxo Complex. *Journal of the American Chemical Society* **1998,** *120* (11), 2652-2653; (c) Goto, Y.; Wada, S.; Morishima, I.; Watanabe, Y., Reactivity of peroxoiron(III) porphyrin complexes: Models for deformylation reactions catalyzed by cytochrome P-450. *Journal of inorganic biochemistry* **1998,** *69* (4), 241-247.

25.   Jo, Y.; Annaraj, J.; Seo, M. S.; Lee, Y. M.; Kim, S. Y.; Cho, J.; Nam, W., Reactivity of a cobalt(III)-peroxo complex in oxidative nucleophilic reactions. *Journal of inorganic biochemistry* **2008,** *102* (12), 2155-9.

26.   Cho, J.; Sarangi, R.; Nam, W., Mononuclear Metal–O2 Complexes Bearing Macrocyclic N-Tetramethylated Cyclam Ligands. *Accounts of Chemical Research* **2012,** *45* (8), 1321-1330.

27.   Sharma, S. K.; May, P. S.; Jones, M. B.; Lense, S.; Hardcastle, K. I.; MacBeth, C. E., Catalytic dioxygen activation by Co(II) complexes employing a coordinatively versatile ligand scaffold. *Chem Commun (Camb)* **2011,** *47* (6), 1827-9.

28.   Corcos, A. R.; Villanueva, O.; Walroth, R. C.; Sharma, S. K.; Bacsa, J.; Lancaster, K. M.; MacBeth, C. E.; Berry, J. F., Oxygen Activation by Co(II) and a Redox Non-Innocent Ligand: Spectroscopic Characterization of a Radical–Co(II)–Superoxide

Complex with Divergent Catalytic Reactivity. *Journal of the American Chemical Society* **2016,** *138* (6), 1796-1799.

29.   Sharma, S. K.; May, P. S.; Jones, M. B.; Lense, S.; Hardcastle, K. I.; MacBeth, C. E., Catalytic dioxygen activation by Co(ii) complexes employing a coordinatively versatile ligand scaffold. *Chemical communications* **2011,** *47* (6), 1827-1829.

30.   Wertz, D.; Valentine, J., Nucleophilicity of Iron-Peroxo Porphyrin Complexes. In *Metal-Oxo and Metal-Peroxo Species in Catalytic Oxidations*, Meunier, B., Ed. Springer Berlin Heidelberg: 2000; Vol. 97, pp 37-60.

31.   Donoghue, P. J.; Gupta, A. K.; Boyce, D. W.; Cramer, C. J.; Tolman, W. B., An Anionic, Tetragonal Copper(II) Superoxide Complex. *Journal of the American Chemical Society* **2010,** *132* (45), 15869-15871.

32.   Pirovano, P.; Magherusan, A. M.; McGlynn, C.; Ure, A.; Lynes, A.; McDonald, A. R., Nucleophilic reactivity of a copper(II)-superoxide complex. *Angewandte Chemie* **2014,** *53* (23), 5946-50.

33.   Wiebe, D. A.; Burton, D. J., Chemoselective halogenation of 2-hydroperfluoroalkyl aldehydes. *Journal of Fluorine Chemistry* **2012,** *139*, 4-11.

34.   Witten, M. R.; Jacobsen, E. N., A Simple Primary Amine Catalyst for Enantioselective α-Hydroxylations and α-Fluorinations of Branched Aldehydes. *Organic Letters* **2015,** *17* (11), 2772-2775.

35.   Masschelein, K. G. R.; Stevens, C. V., Synthesis of 1,1-bisphosphono-2-aza-1,3-dienes, a new class of electron-deficient azadienes. *Tetrahedron Letters* **2008,** *49* (28), 4336-4338.

36.   Yuan, Y.; Shi, X.; Liu, W., Transition-Metal-Free, Chemoselective Aerobic Oxidations of Sulfides and Alcohols with Potassium Nitrate and Pyridinium Tribromide or Bromine. *Synlett* **2011,** *2011* (04), 559-564.

37.   Cunningham, A.; Mokal-Parekh, V.; Wilson, C.; Woodward, S., On the use of mixtures of organotin species for catalytic enantioselective ketone allylation-a detective story. *Organic & Biomolecular Chemistry* **2004,** *2* (5), 741-748.

38.   Buchwald, S. L.; Watson, B. T.; Lum, R. T.; Nugent, W. A., A general method for the preparation of zirconocene complexes of substituted benzynes: in situ generation, coupling reactions, and use in the synthesis of polyfunctionalized aromatic compounds. *Journal of the American Chemical Society* **1987,** *109* (23), 7137-7141.

39.   Cutulic, S. P. Y.; Findlay, N. J.; Zhou, S.-Z.; Chrystal, E. J. T.; Murphy, J. A., Metal-Free Reductive Cleavage of C−O σ-bonds in Acyloin Derivatives by an Organic Neutral Super-Electron-Donor. *The Journal of Organic Chemistry* **2009,** *74* (22), 8713-8718.

40.   (a) Bilgrien, C.; Davis, S.; Drago, R. S., *J. Am. Chem. Soc.* **1987,** *109*, 3786; (b) Bäckvall, J. E.; Chowdhury, R. L.; Karlsson, U., *J. Chem. Soc., Chem. Commun.* **1991**, 473; (c) Lenz, R.; Ley, S. V., *J. Chem. Soc., Perkin Trans. 1* **1997**, 3291; (d) Hanyu, A.; Sakurai, Y.; Fujibayashi, S.; Sakaguchi, S.; Ishii, Y., *Tetrahedron Lett.* **1997,** *38*, 5659.

41.   (a) ten Brink, G. J.; Arends, I. W. C. E.; Hoogenraad, M.; Verspui, G.; Sheldon, R. A., *Adv. Synth. Catal.* **2003,** *345*, 497; (b) ten Brink, G. J.; Arends, I. W. C. E.; Sheldon, R. A., *Adv. Synth. Catal.* **2002,** *344*, 355; (c) Steinhoff, B. A.; Guzei, I. A.; Stahl, S. S., *J. Am. Chem. Soc.* **2004,** *126*, 11268; (d) Sigman, M. S.; Jensen, D. R., *Acc. Chem. Res.* **2006,** *39*, 221.

42.   Trost, B. M.; Masuyama, Y., Chemoselectivity in molybdenum catalyzed alcohol and aldehyde oxidations. *Tetrahedron Letters* **1984,** *25* (2), 173-176.

43.   Jallabert, C.; Riviere, H., Activation de l'oxygene moleculaire par des sels de cuivre monovalent : transformation d'alcools en aldehydes par le systeme CuCl/amine/O2. *Tetrahedron Letters* **1977,** *18* (14), 1215-1218.

44.   Markó, I. E.; Giles, P. R.; Tsukazaki, M.; Brown, S. M.; Urch, C. J., Copper-Catalyzed Oxidation of Alcohols to Aldehydes and Ketones: An Efficient, Aerobic Alternative. *Science* **1996,** *274* (5295), 2044-2046.

45.   (a) Michel, C.; Belanzoni, P.; Gamez, P.; Reedijk, J.; Baerends, E. J., *Inorg. Chem.* **2009,** *48*, 11909; (b) Belanzoni, P.; Michel, C.; Baerends, E. J., *Inorg. Chem.* **2011,** *50*, 11896; (c) Hoover, J. M.; Ryland, B. L.; Stahl, S. S., *J. Am. Chem. Soc.* **2013,** *135*, 2357; (d) Hoover, J. M.; Ryland, B. L.; Stahl, S. S., *ACS Catal.* **2013,** *3*, 2599.

46.   McCann, S. D.; Stahl, S. S., Mechanism of Copper/Azodicarboxylate-Catalyzed Aerobic Alcohol Oxidation: Evidence for Uncooperative Catalysis. *Journal of the American Chemical Society* **2016,** *138* (1), 199-206.

47.   Lee, J. Y.; Peterson, R. L.; Ohkubo, K.; Garcia-Bosch, I.; Himes, R. A.; Woertink, J.; Moore, C. D.; Solomon, E. I.; Fukuzumi, S.; Karlin, K. D., Mechanistic Insights into the Oxidation of Substituted Phenols via Hydrogen Atom Abstraction by a Cupric–Superoxo Complex. *Journal of the American Chemical Society* **2014,** *136* (28), 9925-9937.

48.   Jiang, N.; Ragauskas, A. J., Copper(II)-Catalyzed Aerobic Oxidation of Primary Alcohols to Aldehydes in Ionic Liquid [bmpy]PF6. *Organic Letters* **2005,** *7* (17), 3689-3692.

49.   Suzuki, T.; Morita, K.; Tsuchida, M.; Hiroi, K., Iridium-Catalyzed Oppenauer Oxidations of Primary Alcohols Using Acetone or 2-Butanone as Oxidant. *The Journal of Organic Chemistry* **2003,** *68* (4), 1601-1602.

50.   Piancatelli, G.; Leonelli, F., Oxidation of Nerol to Neral with Iodosobenzene and TEMPO. In *Organic Syntheses*, John Wiley & Sons, Inc.: 2003.